[5] and HSV-1 [11], have been also used for retrograde gene delivery designed for the treatment of injures of the central nervous system, degenerative neural diseases, and motor neuron diseases.

We designed experiments to test whether specific muscles injected with an adenoviral vector could target specific spinal cord segments by retrograde transport more efficiently. The present study was set to answer this question. Specifically, we evaluated the transduction efficacy of AdV-LacZ in cervical, thoracic and lumbar spinal cord segments of rats by immunostaining following injection of the adenoviral vector into candidate target muscles.

The present study was conducted in 63 adult male SD rats (Clea, Tokyo, Japan), aged 8–10 weeks with an average body weight of 264 ± 28.3 g (mean ± S.D.). All animals were housed under a 12-h light:12-h dark cycle in a bacteria-free bio-clean room with free access to food and water. The experimental protocol strictly followed the Fukui University *Ethical Committee Guidelines for Animal Experimentation*.

The Adenovirus Expression Vector Kit (no. 6150; TAKARA Biomedical, Shiga, Japan) was used to produce recombinant adenovirus. To prevent virus replication, bacterial β-galactosidase was subcloned into a cassette cosmid pAxCAwt carrying an adenovirus type-5 genome lacking the E3, E1A and E1B regions. The cosmid pAxCAwt contains a *Swa*I cloning site flanked by a cytomegalovirus enhancer-chicken β-actin hybrid (CAG) promoter on the 5′ end and a rabbit globin poly (A) sequence on the 3′ end. The cosmid was cotransfected into 293 cells with the appropriately cleaved adenovirus DNA–terminal protein complex (COS-TPC method) [14]. The recombinant adenovirus propagated and was later isolated from 293 cells and purified using two rounds of CsCl centrifugation. The final adenovirus titer was 5.0×10^8 plaque forming units/ml. The virus vector protocol strictly followed the Fukui University *Safety Committee Guidelines for Recombinant Virus Experimentation*.

To assess retrograde gene delivery to the spinal cord, rats were first anesthetized with intraperitoneal injection of sodium pentobarbiturate (0.05 mg/g body weight), and the target muscles, (i) sternomastoid, (ii) clavotrapezius, (iii) spinotrapezius, (iv) biceps, (v) triceps, (vi) latissimus dorsi, (vii) thoracoabdominal oblique, (viii) tibialis anterior, and (ix) gastrocnemius were exposed under a surgical microscope. Using a microsyringe, 100 μl AdV-LacZ was carefully injected into the middle belly of the superficial layer of the each muscle. Five rats were used for each transverse section (total 45 rats) and two rats were used for each sagittal section (total 18 rats). These sections were used to evaluate the transduction efficacy and the distribution of X-gal-positively stained cells in the spinal cord. One week after the muscle injection, the rats were anesthetized and the right cardiac auricle was exposed, through anterior thoracotomy, and perfused with 300 ml phosphate buffered saline (PBS; at 4 °C) followed by 200 ml of 2% paraformaldehyde in 0.1 M PBS (pH 7.6). Immediately after perfusion, the spinal cord segment extending between the pyramidal decussation and the S2 segment was removed *en bloc* and stored in 0.1 M PBS containing 20% sucrose at 4 °C for 36 h. Tissue blocks were embedded in Tissue-Tek (OCT Compound 4583, Sakura Finetechnical, Tokyo) and stored frozen at −80 °C. Using a cryostat, serial 50 μm-thick transverse and sagittal frozen sections were prepared for each rat, serially mounted on glass slides and fixed with 2% paraformaldehyde in 0.1 M PBS. The transverse sections were divided into two groups by collecting every second section separately for X-gal staining and Nissl staining. The transduction efficacy was calculated using the formula: number of X-gal-stained cells/number of Nissl-stained cells × 100 (%). On the other hand, to assess the expression of AdV-LacZ gene in other body organs, we removed the lung, liver, kidney, and diaphragm for similar analysis.

To detect β-galactosidase activity (X-gal staining) in the spinal cord, fresh frozen sections stained with X-gal reagent (2% 5-bromo-4-chloro-3-indolyl-β-D-galactopyranoside; in dimethylformamide, β-galactosidase Staining Kit, Mirus, Madison, WI) were stored in a 37 °C thermostat container for 24 h to produce a blue color in β-galactosidase-expressing cells. Using a microscope, large multipolar cell bodies with excessive cytoplasm in the anterior horn were counted as viable motoneurons. Cell counting was conducted by two independent observers. The numbers of X-gal-positive cells per cross-section at each segment were counted to quantify the level of expression. We evaluated the surviving motoneurons using Nissl staining with cresyl violet, in exactly the same manner as described previously [2,18]. Nissl-positive cells were counted in a manner similar to that described for X-gal staining. The transduction efficacy was calculated in a manner similar to the procedure described above. Data were expressed as mean ± S.D.

Figs. 1–3 show the distribution of X-gal-stained neuronal cells in the spinal cord following delivery of AdV-LacZ through the indicated muscles. In the cervical spinal cord (Fig. 1), the sternomastoid and clavotrapezius muscles were the most appropriate target organs with high transduction efficacy (77.4–93.1%) at each cervical segment. Although a high transduction efficacy was also noted for the latissimus dorsi and thoracoabdominal oblique muscles (69.6–89.6%), the reproducibility was lower than that of the above two muscles. Although X-gal-stained cells were identified in C5-7 following AdV-LacZ injection into the spinotrapezius, biceps, and triceps muscles, the transduction efficacy and activity were low (<50.3%). Furthermore, only a few X-gal-stained cells were noted following injection of AdV-LacZ into the tibialis anterior and gastrocnemius muscles. In the thoracic spinal cord (Fig. 2), fewer anterior horn motoneurons were X-gal-stained compared with the cervical spinal cord. Although X-gal-stained cells were identified following injection of AdV-LacZ into the latissimus dorsi and thoracoabdominal oblique muscles with moderate transduction efficacy (46.5–78.3%), reproducibility was uneven. In the lumbar spinal cord (Fig. 3), the transduction efficacy was highest through the tibialis anterior and gastrocnemius muscles (56.6–78.3%), followed by all other muscles except the biceps and triceps muscles (48.3–67.6%).

Fig. 4 shows LacZ gene expression in other organs. Although X-gal-stained cells were noted in the dorsal root ganglion, the number of positively stained cells in the posterior horn was less than in the anterior horn (Fig. 4a and b). No X-gal-stained

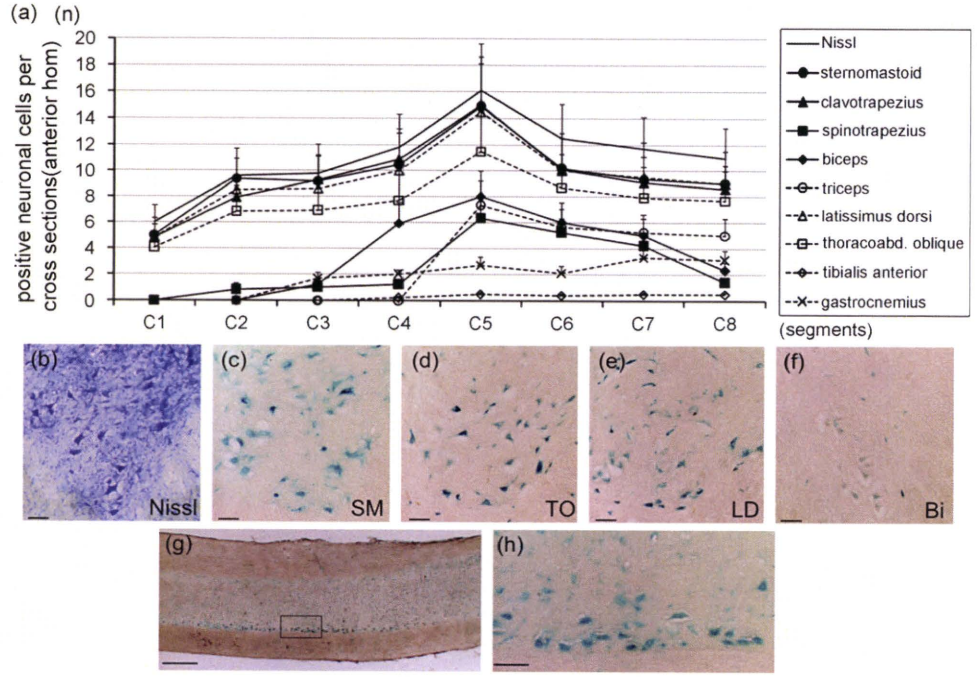

Fig. 1. (a) Number of X-gal-stained anterior horn cells per cross-section of cervical spinal cord segments according to delivery organ. Data are mean ± S.D. (b–f) Transverse sections of the spinal cord at C5 level; magnification ×100, Scale bar = 100 μm. (b) Nissl staining (c–h) X-gal staining, 1 week after injection through (c) sternomastoid, (d) thoracoabdominal oblique, (e) latissimus dorsi, and (f) biceps muscles. (g) Parasagittal section of the cervical spinal cord, 1 week after injection through the sternomastoid muscle; magnification ×10, Scale bar = 1 mm. (h) High-power photomicrograph of the box area in (g) (C5 area); magnification ×100, Scale bar = 100 μm.

cells were detected in the lungs, liver, kidneys and diaphragm (Fig. 4c–f).

The location of corticospinal motoneurons can be visualized in the spinal cord in relation to the muscles they innervate [1,12]. In our study, gene expression was noted mainly around the area of innervation in the spinal cord. Although X-gal-stained cells were also found in other spinal cord levels but their distribution showed no anatomical basis. These results suggest that the ade-

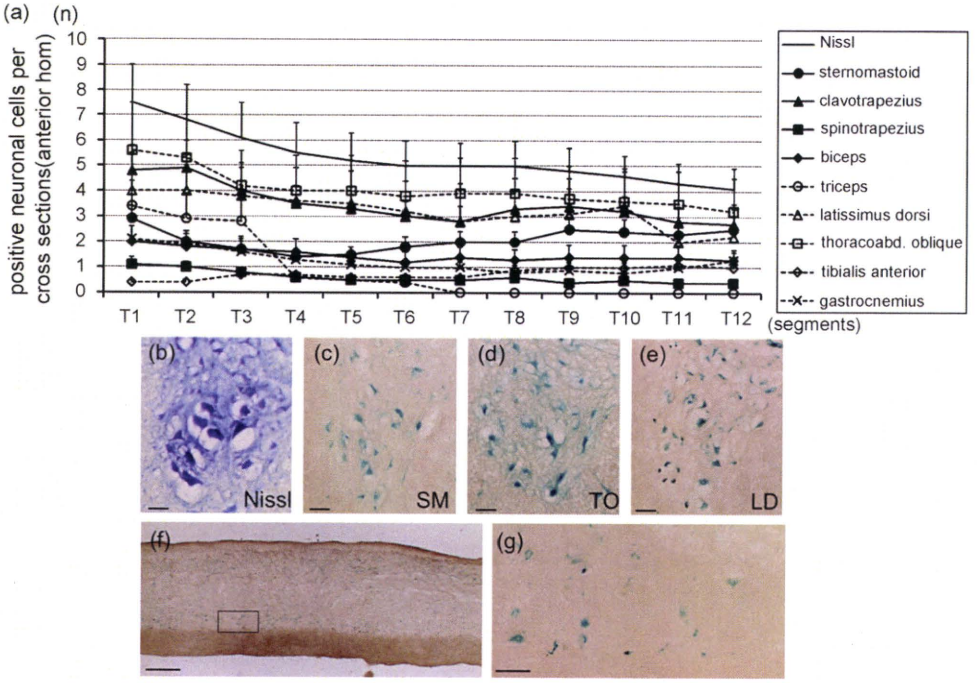

Fig. 2. (a) Number of X-gal-stained anterior horn cells per cross-section of thoracic spinal cord segments according to delivery organ. Data are mean ± S.D. (b–e) Transverse sections of the spinal cord at T8 level; magnification ×100, Scale bar = 100 μm. (b) Nissl staining (c–g) X-gal staining, 1 week after injection through (c) sternomastoid, (d) thoracoabdominal oblique, and (e) latissimus dorsi muscles. (f) Parasagittal section of the thoracic spinal cord, 1 week after injection through the thoracoabdominal oblique muscle; magnification ×10, Scale bar = 1 mm. (g) High-power photomicrograph of the box area in (f) (T8 area); magnification ×100, Scale bar = 100 μm.

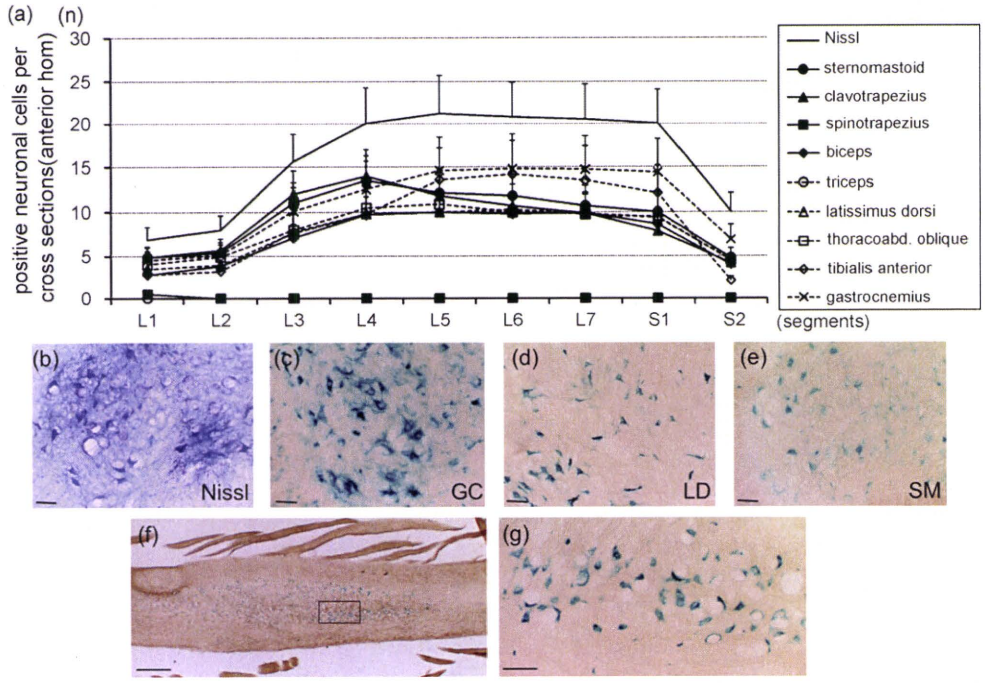

Fig. 3. (a) Number of X-gal-stained anterior horn cells per cross-section of lumbar spinal cord segments according to delivery organ. Data are mean ± S.D. (b–e) Transverse sections of the spinal cord at L5 level; magnification ×100, Scale bar = 100 μm. (b) Nissl staining (c–g) X-gal staining, 1 week after injection through (c) gastrocnemius, (d) latissimus dorsi, (e) and sternomastoid muscles. (f) Parasagittal section of the lumbar spinal cord, 1 week after injection through the tibialis anterior muscle; magnification ×10, Scale bar = 1 mm. (g) High-power photomicrograph of the box area in (f) (L5 area); magnification ×100, Scale bar = 100 μm.

novirus vector is a strong retrograde tracer and could potentially transduce spinal cord neurons with high efficacy.

The transduction efficacy of the tested muscles varied considerably. While the reason for the variability was not investigated in the present study, we postulate it could be due to differences in (i) length of axons to the spinal cord (biceps and triceps may a long distant from the spinal cord), (ii) volume of the target organ (transduction efficacies of latissimus dorsi and thoracoabdominal oblique muscles were uneven probably due to the sheet-like broad muscles), (iii) variation in motoneuron innervation (presence of multiple innervating motoneurons may be not appropriate for retrograde gene transduction), (iv) differences in the density/compaction of motor endplates in the belly of the muscles (such differences may explain the lower efficacy via upper limb muscles compared with lower limb muscles, and the uneven efficacy via the trunk muscles).

The efficiency of retrograde delivery of neuropeptide genes could be influenced by various factors, such as [7]: local secretion of proteins from AdV-infected muscles, uptake and retrograde axonal transport of AdV in motoneurons, and secretion of proteins in AdV-infected muscles into the systemic circulation. Our results suggested that AdV-LacZ is transported via retrograde axoplasmic flow through axons, but not through the systemic circulation because no gene expression was noted in the examined body organs. Retrograde gene delivery may be potentially more advantageous than direct gene administration into the spinal cord in terms of safety, repeated administration, ease of use, and reduction of inflammatory response in the neural tissue [4,16].

Table 1 shows the most appropriate target organs for cervical and lumbar spinal cord gene delivery, based on the results of the present study. In this regard, cervical and lumbar spinal cords have intumescences around C5 and L5 [1], and only a small num-

Table 1
Target organs and transduction efficacy for delivery of adenoviral vector to cervical and lumbar spinal cord segments by retrograde gene delivery

Spinal cord area	Target organ (transduction efficacy)
Upper-middle cervical spinal cord	Sternomastoid muscle (80.6–93.1%)
Middle-lower cervical spinal cord	Clavotrapezius muscle (77.4–92.5%) Latissimus dorsi muscle (67.1–78.3%)
Thoracic spinal cord[a]	Thoracoabdominal oblique muscle (46.5–74.1%) Tibialis anterior muscle (56.6–70.2%)
Lumbar spinal cord	Gastrocnemius muscle (67.9–78.3%)

[a] Retrograde gene delivery to the thoracic spinal cord may be unsuitable compared with the cervical and lumbar spinal cord, probably due to the small number of anterior horn neurons.

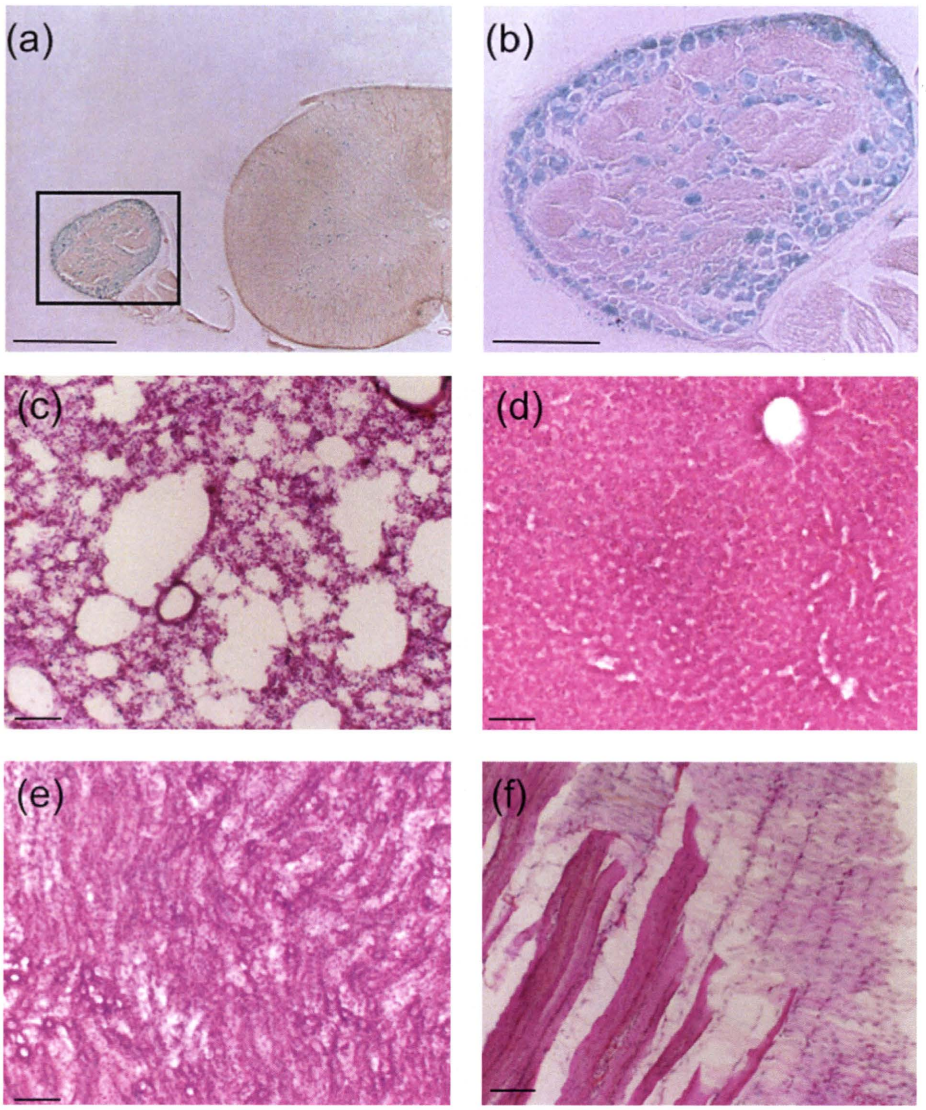

Fig. 4. Immunostaining for LacZ gene (X-gal staining) in various organs. (a) Spinal cord and dorsal root ganglion (C5 level); magnification ×10, Scale bar = 1 mm. (b) High-power photomicrograph of the box area in (a) (dorsal root ganglion); magnification ×100, Scale bar = 100 μm. (c) Lung, (d) liver, (e) kidney, (f) diaphragm; magnification ×40, Scale bar = 100 μm.

ber of anterior horn neurons are present in the thoracic spinal cord. Based on these anatomical features, retrograde gene delivery to the thoracic spinal cord may be unsuitable to produce the desired neuroprotective effects.

In conclusion, retrograde delivery of β-galactosidase gene, using adenoviral vector, to the cervical and lumbar spinal cord segments seems feasible by injection into the appropriate target organ. Adenovirus vector is an efficient retrograde tracer since it can deliver the carried gene to a wide area of the spinal cord and not to other body organs.

Acknowledgments

This work was supported by a Grant-in-Aid (grant nos. 19791023) for General Scientific Research from the Ministry of Education, Culture, Sports, Science and Technology of Japanese Government.

References

[1] J. Altman, S.A. Bayer (Eds.), Motoneuron Columns and Subcolumns. Development of the Human Spinal Cord: An Interpretation Based on Experimental Studies in Animals, Oxford, 2001, pp. 42–61.
[2] H. Baba, Y. Maezawa, S. Imura, N. Kawahara, K. Nakahashi, K. Tomita, Quantitative analysis of the spinal cord motoneuron under chronic compression: an experimental observation in the mouse, J. Neurol. 243 (1996) 109–116.
[3] A. Blesch, P. Lu, M.H. Tuszynski, Neurotrophic factors, gene therapy, and neural stem cells for spinal cord repair, Brain Res. Bull. 57 (2002) 83–88.
[4] N.M. Boulis, D.E. Turner, M.J. Imperiale, E.L. Feldman, Neuronal survival following remote adenovirus gene delivery, J. Neurosurg. (Spine) 96 (2002) 212–219.
[5] N.M. Boulis, N.E. Willmarth, D.K. Song, E.L. Feldman, Intraneural colchicines inhibition of adenoviral and adeno-associated viral vector remote spinal gene delivery, Neurosurgery 52 (2003) 381–387.
[6] P. Dergham, B. Ellezam, C. Essagian, H. Avedissian, W.D. Lubell, L. McKerracher, Rho signaling pathway targeted to promote spinal cord repair, J. Neurosci. 22 (2002) 6570–6577.

[7] G. Haase, B. Pettmann, E. Vigne, L. Castelnau-Ptakhine, H. Schmalbruch, A. Kahn, Adenovirus-mediated transfer of the neurotrophin-3 gene into skeletal muscle of *pmn* mice: therapeutic effects and mechanisms of action, J. Neurol. Sci. 160 (1998) S97–S105.

[8] W.T. Hendriks, M.J. Ruitenberg, B. Blits, G.J. Boer, J. Verhaagen, Viral vector-mediated gene transfer of neurotrophins to promote regeneration of the injured spinal cord, Prog. Brain Res. 146 (2004) 451–476.

[9] W.T. Hermens, J. Verhaagen, Viral vectors, tools for gene transfer in the nervous system, Prog. Neurobiol. 55 (1998) 399–432.

[10] B.K. Kaspar, D. Erickson, D. Schaffer, L. Hinh, F.H. Gage, D.A. Peterson, Targeted retrograde gene delivery for neuronal protection, Mol. Ther. 5 (2002) 50–56.

[11] S.D. Keir, W.J. Mitchell, L.T. Feldman, J.R. Martin, Targetting gene expression in spinal cord motor neurons following intramuscular inoculation of an HSV-1 vector, J. Neurol. Virol. 1 (1995) 259–267.

[12] S. Kitamura, A. Sakai, A study on the localization of the sternocleidomastoid and trapezius motoneurons in the rat by means of the HRP method, Anat. Rec. 202 (1982) 527–536.

[13] J.W. Mcdonald, X.Z. LIU, Y. QU, S. Liu, S.K. Mickey, D. Turetsky, D.I. Gottlie, D.W. Choi, Transplanted embryonic stem cells survive, differentiate and promote recovery in injured rat spinal cord, Nat. Med. 4 (1999) 291–297.

[14] S. Miyake, M. Makimura, Y. Kanegae, S. Harada, Y. Sato, K. Takamori, C. Tokuda, I. Saito, Efficient generation of recombinant adenoviruses using adenovirus DNA–terminal protein complex and a cosmid bearing the full-length virus genome, Proc. Natl. Acad. Sci. U.S.A. 93 (1996) 1320–1324.

[15] H. Nakajima, K. Uchida, S. Kobayashi, T. Inukai, Y. Horiuchi, T. Yayama, R. Sato, H. Baba, Rescue of rat anterior horn neurons after spinal cord injury by retrograde transfection of adenovirus vector carrying brain-derived neurotrophic factor gene, J. Neurotrauma 24 (2007) 703–712.

[16] H. Nakajima, K. Uchida, S. Kobayashi, Y. Kokubo, T. Yayama, R. Sato, H. Baba, Targeted retrograde gene delivery into the injured cervical spinal cord using recombinant adenovirus vector, Neurosci. Lett. 385 (2005) 30–35.

[17] L.N. Novikova, L.N. Novikov, J.O. Kellerth, Brain-derived neurotrophic factor reduces necrotic zone and supports neuronal survival after spinal cord hemisection in adult rats, Neurosci. Lett. 220 (1996) 203–206.

[18] K. Uchida, H. Baba, Y. Maezawa, S. Furukawa, N. Furusawa, S. Imura, Histological investigation of spinal cord lesions in the spinal hyperostotic mouse (twy/twy): morphological changes in anterior horn cells and immunoreactivity to neurotropic factors, J. Neurol. 245 (1998) 781–793.

[19] K. Xu, K. Uchida, H. Nakajima, S. Kobayashi, H. Baba, Targeted retrograde transfection of adenovirus vector carrying brain-derived neurotrophic factor gene prevents loss of mouse (twy/twy) anterior horn neurons in vivo sustaining mechanical compression, Spine 31 (2006) 1867–1874.

SPINE Volume 33, Number 24, pp 2596–2604

Gene Expression Profiles of Neurotrophic Factors in Rat Cultured Spinal Cord Cells Under Cyclic Tensile Stress

Kenzo Uchida, MD, DMSc,* Hideaki Nakajima, MD, DMSc,* Takaharu Takamura, MD,* Shoei Furukawa, PhD,† Shigeru Kobayashi, MD, DMSc,* Takafumi Yayama, MD, DMSc,* and Hisatoshi Baba, MD, DMSc*

Study Design. An experimental study to investigate the *in vitro* gene expression of neurotrophic factors and receptors in cultured rat spinal cord cells subjected to cyclic mechanical stretch forces.

Objective. We evaluated *in vitro* expression of neurotrophic factors and receptors in cultured rat spinal cord cells under cyclic tensile stress.

Summary of Background Data. Application of compressive mechanical stress to the spinal cord results in multiple changes making it difficult to examine the expression of neurotrophic factors and their receptors. There are no *in vitro* studies that investigated the biologic responses of cultured spinal cord cells to tensile stress.

Methods. Spinal cord cells were isolated for culture from 15-day Sprague-Dawley rat embryos. We used the FX3000 Flexercell Strain Unit to induce mechanical stress. We analyzed the effects of mechanical stress on cell morphology, mRNA expression levels of various neurotrophic factors, and their immunoreactivities at 0, 2, 6, 12, 24, and 36 hours.

Results. Tensile stress for 6 hours resulted in reduction of spinal cord cells and loss of neurites. Cells that survived 24-hours stress showed swollen irregular-shaped soma, bleb formation, and fragmented neurites. The cell survival rate decreased, whereas lactate dehydrogenase release increased significantly at 6 hours. There were significant increases in mRNA expression levels of nerve growth factor, brain-derived neurotrophic factor, trkB, p75 neurotrophin receptor ($p75^{NTR}$), glial cell line-derived neurotrophic factor, and caspase-9 during the early period after application of tensile stress.

Conclusion. Our results suggest survival of spinal cord neuronal cells under injurious tensile stress with increased synthesis and utilization of several neurotrophic factors, receptors, and expression of proteins related to cell apoptosis.

Key words: tensile stress, neurotrophic factor, cultured cell, neuron, rat, spinal cord. **Spine 2008;33: 2596–2604**

The spinal cord and neurons are always subjected to mechanical stress including tensile stresses, and during spine movement, such stress may be applied to the spinal cord in a very complex manner in association with subsequent symptomatic manifestation.[1,2] In addition, mechanical (tensile) stress to the spinal cord may ultimately cause motoneuron dysfunction and axonal degeneration.[3,4] Longitudinal vertebral distraction and the physiologic tension zone[5] of the spinal cord are closely correlated with each other when the spine is subjected to flexural positioning[6,7] and excessive kyphosis in the thoracic vertebrae.[8] Clinically, application of excessive and/or repetitive longitudinal tensile stress to spinal cord neurons may result in loss of biologic activities, as occurs in tethered cord syndrome and acute and chronic spinal cord injuries.[5] Furthermore, a high-magnitude tensile stress may result in damage of cervical motoneurons, in association with compression, shearing, and distraction damage to the cord.[5,6] Tensile stress applied to the spinal cord is thus potentially critical and linked to subsequent neuronal damage, but it is extremely difficult to estimate the isolated effect of tensile stress in the *in vivo* experimental setting.

Interestingly, application of mechanical force to the spinal cord results in loss of function in some neurons, whereas others show increased metabolic activity to resist injury. It is conceivable that mechanical stress of the spinal cord induces both neuronal survival and repair, or cell death. Recent studies of experimental spinal cord damage in animals examined the function, source, and dynamics of induction of endogenous neurotrophic factors, including brain-derived neurotrophic factor (BDNF), neurotrophin (NT)-3, and their receptors,[9–15] that are essential for neuronal survival, repair, and neurite outgrowth and arborization. However, in these experiments, excess mechanical stress could have caused tissue or cell reactions such as activation of glial cells or invasion of foreign cells from the periphery. It could have also induced various pathologic events and release of

From the *Department of Orthopaedics and Rehabilitation Medicine, Fukui University Faculty of Medical Sciences, Fukui; and †Laboratory of Molecular Biology, Gifu Pharmaceutical University, Gifu, Japan.
Acknowledgement date: April 2, 2008. Revision date: July 4, 2008. Acceptance date: July 9, 2008.
The manuscript submitted does not contain information about medical device(s)/drug(s).
No funds were received in support of this work. No benefits in any form have been or will be received from a commercial party related directly or indirectly to the subject of this manuscript.
This work was supported in part by Grant-in-Aid (to H.B. and K.U.) for General Scientific Research of the Ministry of Education, Science and Culture of Japan (grants 12470305, 13671499, 15591571, 16390435, and 18390411). This work was also supported in part by grants (to H.B.) from the Investigation Committee on Ossification of the Spinal Ligaments, Public Health Bureau of the Japanese Ministry of Health and Welfare (2005–2007).
Address correspondence and reprint requests to Kenzo Uchida, MD, DMSc, Department of Orthopaedics and Rehabilitation Medicine, Fukui University Faculty of Medical Sciences, Shimoaizuki 23, Matsuoka, Fukui 910-1193, Japan; E-mail: kuchida@u-fukui.ac.jp

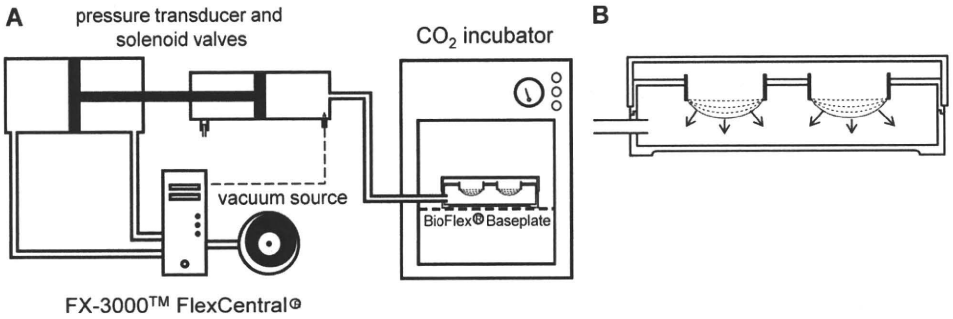

Figure 1. The FX3000 Flexercell Strain Unit. Schematic drawing of the apparatus used for cell stimulation using cyclic tensile strain (**A**). The flexible bottom of the culture plates (BioFlex Base plate) could be stretched under vacuum (**B**).

inflammatory mediators that could have positively or negatively influenced spinal cord function.[16] The complexity of the *in vivo* situation may result in a limited accessibility to the tissue of interest, preventing real-time and spatial measurement of biologic or mechanical parameters.[17] Thus, to gain a better understanding of the neuronal response to spinal movement and physiologic state, *in vitro* models of spinal cord stress could perhaps allow a better control of the extracellular environment, easy and perhaps repeated access to the cells, and help elucidate the mechanisms of response to mechanical stimuli.

To our knowledge, there are no studies that examined the biologic and immunohistochemical responses of spinal cord cultured cells to mechanical tensile stress. Flexercell Strain Unit (FX3000; Flexercell International, Hillsborough, NC) is a cell-stretching apparatus that allows application of cyclic tensile force to cultured cells. The system has been used to elucidate the mechanism of mechanical signal in various types of cells.[18–20] The present study was designed to assess the effect of cyclic mechanical tensile force on the expression and synthesis of neurotrophic factors and their receptors in cultured spinal cord cells with the use of this equipment.

■ Materials and Methods

Cell Cultures

Primary cell cultures were established using the method described previously.[21,22] In brief, spinal cords of Sprague-Dawley rat embryos were dissected out at postcoital day 15 and stripped of the dorsal root ganglions and the meninges. Dissected tissues were rinsed with cold Ca^{+2}- and Mg^{+2}-free Hanks balanced salt solution (HBSS) supplemented with 4 g/L glucose, and incubated at 37°C for 20 minutes with 0.03% (w/v) trypsin solution in HBSS with mild shaking. They were transferred into HBSS containing 0.1% (w/v) soybean trypsin inhibitor (Sigma, St. Louis, MO) and 0.2% (w/v) bovine serum albumin and triturated very mildly. The cell suspension was filtered through nylon mesh (70 μm, Cell Strainer; Becton Dickinson, Bedford, MA). The culture medium consisted of 75-mL Leibovitz's L-15 medium supplemented with glucose (4 g/L), 1.0 mL N2 supplement, 15-mL 0.15 M sodium bicarbonate, 10-mL heat-inactivated horse serum, 1 mL of 100 mmol/L L-cysteine, and 1-mL penicillin G 10^4 U/mL and neutralized with CO_2. After centrifugation at 400*g* for 15 minutes at 4°C, the precipitated cells were gently resuspended in a fresh culture medium and plated at a density of 4.0×10^5 cells/well onto a 6-well culture plate with a flexible-polystyrene bottom coated with type IV collagen (BioFlex Baseplate, Flexercell International).

The experiment was carried out in the Orthopedic Spinal Cord Laboratory of Fukui University. The experimental protocol strictly followed the Ethics Review Committee Guidelines for Animal Experimentation of our University Medical Faculty.

Application of Tensile Stress to Cultured Spinal Cord Cells

The cell stretching device used in this study was Flexercell FX3000. The device consists of a computer-controlled vacuum unit (Figure 1A), a culture plate with a flexible-polystyrene well-bottom coated with type IV collagen (BioFlex Baseplate) (Figure 1B), and another culture well plate with a nondeformable culture well bottom constructed of the same material. The culture plates consisted of 6-well (35-mm diameter) flexible-bottomed culture plate with a hydrophilic surface. Application of vacuum provides a hemispherically downward deforming force to the flexible bottom, resulting in a nonhomogenous strain profile with a maximum at the periphery and a geometric decline toward zero at the center of the culture well bottom. The cells were placed in the culture well plates at an average density of 4.0×10^5 cells/well. For these experiments, spinal cord cells in the culture were subjected to cycles of 1 second of a maximum 12% elongation (vacuum level, 10.3 kPa). Panjabi and White[5] demonstrated that the elastic properties of the cervical spinal cord are dramatically altered when it is subjected to approximately 10% elongation. In our previous *in vivo* study,[6] the amplitude of epidurally recorded spinal cord evoked potentials began to diminish, especially the second component (N2 spike), when the longitudinal length of the cord shortened by 10% to 17%. Thus, in the present study, we set the tensile stress at a maximum 12% elongation. The flexible-bottomed culture plates including the control plates were then placed on the vacuum baseplate in the incubator (37°C in 5% CO_2). After 3 days of cell seeding, cells were subjected to cyclic stretch stress for 48 hours. Repeated examinations by phase microscopy (IX70, Olympus, Tokyo, Japan) showed that the cells remained attached to the substratum during elongation. The cells were observed morphologically after application of tensile stress and various assays, quantification of mRNA expression of neurotrophic factors, and immunoreactivity were conducted at 0, 2, 6, 12, 24, and 36 hours after the application of tensile stress.

Assessment of Cell Survival and Cell Damage

To determine possible cellular damage due to tensile stress, cell survival was examined by manual cell counting and by measurement of lactate dehydrogenase (LDH) release at 0, 2, 6, 12, 24, and 36 hours after the application of tensile stress. Calcein-acetoxymethyl ester (calcein-acetoxymethyl: 3.00 μmol/L) was

Table 1. Sequences of Primers Used for Real-Time PCR

Target Protein	Forward Primer	Reverse Primer	PCR Product Size (bp)	Sequence Accession No.
NGF	5H'-CCATGTGGTTCCTGATCCTGTTC-3'	5'-TCCAACAACCCGAGACTGGAC-3'	83	NM031523
BDNF	5'-TCCTGATAGTTCTGTCCATTCAGCA-3'	5'-GCCATTCATTCAGGCTTCCA-3'	93	NM012513
NT-3	5'-CATGTCGACGTCCCTGGAAATAG-3'	5'-TGGACATCACCTTGTTCACCTGTAA-3'	82	NM031073
NT-4/5	5'-GAGGTGGAGGTGCTGTTGAC-3'	5'-TCCCACTCAGGAGCCAGAA-3'	150	NM013184
trk A	5'-CAAGATGCTGGTGGCTGTCAA-3'	5'-AGCAGCTCTGCCTCACGATG-3'	81	NM021589
trk B	5'-CCTTGACCGATCTGGCTTCTGTA-3'	5'-TAGTTGTGGTGGGCAAACTGGA-3'	107	NM012731
trk C	5'-CATGAAGCATGGAGACCTGAACA-3'	5'-ACCATGCCGGAGGCTATCTG-3'	147	NM019248
$p75^{NTR}$	5'-AGGGCTGGTCCATTGGTCTATTC-3'	5'-TTAAGGGCCGTGTTGGCTTC-3'	132	NM012610
GDNF	5'-CCGGACGGGACTCTAAGATGA-3'	5'-GTCAGGATAATCTTCGGGCATATTG-3'	194	NM019139
GFRα-1	5'-GGGACGCTTTGGTGTCTGAA-3'	5'-CCAGGTACACTTGGATGTTGGATG-3'	132	NM012959
Caspase-3	5'-GCAGCAGCCTCAAATTGTTGACTA-3'	5'-TGCTCCGGCTCAAACCATC-3'	144	NM012922
Caspase-9	5'-CTGAGCCAGATGCTGTCCCATA-3'	5'-CCAAGGTCTCGATGTACCAGGAA-3'	168	NM031632
GAPDH	5'-GGCACAGTCAAGGCTGAGAATG-3'	5'-ATGGTGGTGAAGACGCCAGTA-3'	143	NM017008

used to identify living cells (Live/Dead Assay; Molecular Probes, Eugene, OR). Calcein-acetoxymethyl is a membrane-permeable dye that is cleaved by intracellular esterase to produce an impermeant green-wavelength fluorophore in living cells.[23,24] The culture medium was removed, and the cells were then washed twice with PBS and stained for 75 minutes at 32°C. The numbers of attached living (green) cells in at least 6 high-power fields (each containing at least 100 cells) were counted using fluoromicroscopy (IX70; Olympus) and a color image analyzer (MacSCOPE; Mitani, Fukui, Japan) in more than 3 wells for each time point. The cell survival rate (%) was calculated relative to the cell number at 0 hour. Because spinal cord cells do not proliferate, the cell counts were almost uniform and at a density from 3.3×10^5 to 4.8×10^5 cells/well during 3 days after dissemination on Bioflex Baseplate in the absence of tensile stress.

LDH, a stable enzyme present in the cytoplasm of all cells, is rapidly released into the culture medium after damage to the plasma membrane. The culture medium was sampled at the aforementioned time points after mechanical stimulation and analyzed using the CytoTox-ONE kit (Promega, Madison, WI). This assay has been used to discriminate between apoptotic and necrotic cell death.[25,26] After incubation of the cells with the reagent, each reaction was stopped by stop solution provided with the kit to prevent further generation of fluorescent product. LDH release was assessed using a chemiluminescence imaging analyzer (IS-8000-OH; Alpha Innotech, San Leandro, CA) in more than 3 wells for each time point. LDH release was almost uniform in the absence of stress during 2 days after dissemination on Bioflex Baseplate. LDH release rate (%) after mechanical stress was calculated per volume and expressed relative to that at 0 hour.

Real-Time Reverse Transcription Polymerase Chain Reaction

The gene expressions of nerve growth factor (NGF), BDNF, NT-3, NT-4/5, trkA, trkB, trkC, p75 NT receptor ($p75^{NTR}$), glial cell line-derived neurotrophic factor (GDNF), GDNF family receptor (GFR)-α1, caspase-3, and caspase-9 were examined by real-time polymerase chain reaction (RT-PCR) at each time point after mechanical stimulation. Briefly, the cultured cells on each well were disrupted in a lysis buffer containing β-mercaptoethanol, and total RNA was purified using RNeasy Mini Kit (Qiagen, Valencia, CA) and treated with DNase I (Takara Biomedicals, Kyoto, Japan). Reverse transcription was performed using 1 μg of total RNA, AMV reverse transcriptase XL (Takara Biomedicals, Ohtsu, Japan) and random primer. Real-time PCR was performed on Prism 7000 (ABI) using 1 μL of the synthesized cDNA and SYBR Green PCR master mix (Applied Biosystems, Foster, CA). Table 1 lists the primer sequences used in this study. The target genes were amplified and analyzed in triplicate using ABI Prism 7000 SDS Software (Applied Biosystems). The expression levels of target genes were compared with that of glyceraldehyde-3-phosphate dehydrogenase at each time, and the expression levels of target genes were calculated relative to that of glyceraldehyde-3-phosphate dehydrogenase.

Immunohistochemical Analysis

Neuronal survival under cyclic tensile stress was determined by manual cell counting of NeuN-labeled cells using a fluorescence microscope. A round flexible bottom well (35 mm in diameter) was divided into 6 sectors; the cutting bottom attached cultured cells was used as a section during the immunocytochemical procedure. After application of tensile stress, the cultured spinal cord cells were washed twice with PBS and fixed in 2% paraformaldehyde for 15 minutes and then incubated at room temperature for 10 minutes in BlockAce (UK-B25, Snow-Brand, Tokyo) to prevent nonspecific reactions. Cells were processed for immunocytochemical detection of NeuN by incubation with mouse antibody to NeuN (1:400; Chemicon International, Temecula, CA) for 20 hours at 4°C, followed by incubation with goat antimouse Alexa Flour 488/fluorescein-conjugated antibody (1:400; Molecular Probes, Eugene, OR) for 1 hour at room temperature. Sections were counterstained with nuclear marker 6-diamidino-2-phenylindole (DAPI) (Abbott Molecular, Des Plaines, IL). The immunostained cells were visualized under a fluorescence microscope (AX80, Olympus) with U-MNIBA cube (BP460–490 nm excitation and BA515–550 nm emission) and U-MWU cube (BP330–385 nm excitation and BA420 nm emission). DAPI-labeled and double-labeled cells in at least 6 high-power fields (magnification, ×100), each containing at least 10 cells, were counted in more than 3 wells at each time point. The ratio of DAPI-labeled cell count and NeuN-labeled cell count was calculated automatically, using a color image analyzer (Mitani), which represented neuronal survival rate (%) at each time point.

For identification of immunoreactivity to neurotrophic factors and their receptors in neurons after incubation with mouse NeuN antibody and goat antimouse Alexa 488, the cells were incubated with rabbit antibody to NGF (1:400; Santa Cruz Biotechnology, Santa Cruz, CA), or with rabbit antibody to BDNF (Chemicon International), or with rabbit antibody to $p75^{NTR}$ (1:400; Santa Cruz Biotechnology), or rabbit antibody

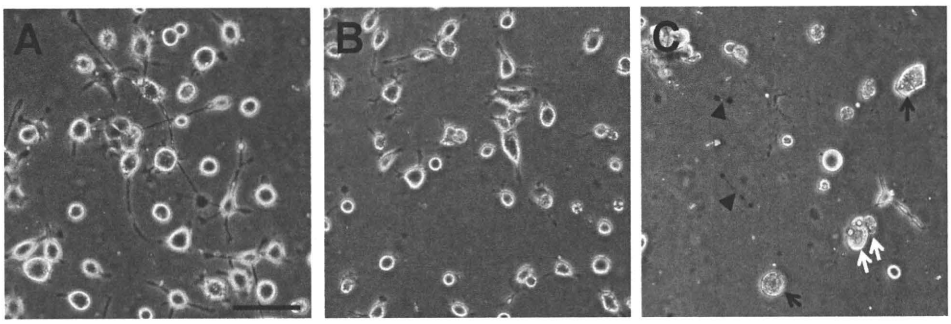

Figure 2. Phase contrast photomicrographs showing morphologic changes in primary cultured spinal cord cells at 0 hour (**A**), 6 hours (**B**), and 24 hours (**C**) after application of cyclic mechanical tensile stress. Decrease in the number of cells and loss of neurites are evident 6 hours after application of tensile stress (**B**) compared to controls (**A**). Cultured cells had irregularly shaped swollen somatic bodies (black arrows) and blebs (white arrows) and showed fragmentations of neurites (arrow heads) 24 hours after stress application (**C**). Scale bar = 100 μm.

to GDNF (1:400; Santa Cruz Biotechnology). The cells were subsequently incubated with goat antirabbit antibody Alexa Flour 594/fluorescein-conjugated antibody (1:400; Molecular Probes) and counted using a confocal microscope equipped with a 15-mWatt krypton argon laser (TCS SP2; Leica Instruments, Nusslosh, Germany). The 488- and 543-nm lines of an argon/helium-neon laser were used for fluorescence excitation.

Statistical Analysis

All values are expressed as mean ± SEM. Differences between values at a particular time and those of the corresponding control were tested by 1-way ANOVA and Tukey *post hoc* test. A P less than 0.05 denoted the presence of a statistically significant difference. The above tests were conducted using SPSS software version 11.0 (SPSS, Chicago, IL).

■ Results

Effects of Cyclic Tensile Stress on Cell Morphology and Cell Survival

Under phase contrast microscopy, the control spinal cord cells (no application of tensile stress) had smooth oval-shaped cell soma (Figure 2A). Application of tensile stress for ≥6 hours decreased the number of spinal cord cells and resulted in loss of neurites, compared to baseline findings (Figure 2B). Application of tensile stress for 24 hours resulted in swelling of the remaining cells with irregularly shaped cell soma and appearance of several blebs within the cells, together with fragmentation of some neurites (Figure 2C).

The cell survival rate as assessed by manual counting of the number of living cell decreased in a time-dependent manner under cyclic tensile stress, from 74% ± 22% at 2 hours to 53% ± 16% at 6 hours, 48% ± 11% at 12 hours, 40% ± 12% at 24 hours, and 38% ± 7% at 36 hours (Figure 3A). The decrease in the number of living cells became significant after 6 hours. On the other hand, LDH release in the culture medium increased at 6 hours and reached a plateau over the subsequent 12 hours (Figure 3B). The time course of changes in LDH release correlated with the morphologic changes seen in mechanically stressed cells.

Effects of Cyclic Tensile Stress on Neuronal Survival

Among DAPI-labeled cells, 71% cells were positive for NeuN before the application of tensile stress 3 days after plating. Neuronal survival rate decreased in a time-dependent manner when cells were under cyclic tensile stress, from 71% ± 10% at 0 hour (before application of tensile stress), to 40% ± 15% at 2 hours of application, 22% ± 9% at 6 hours, 18% ± 7% at 12 hours, 12% ± 4% at 24 hours, and 10% ± 3% at 36 hours, compared to nonstress cells at each time point (Figure 4).

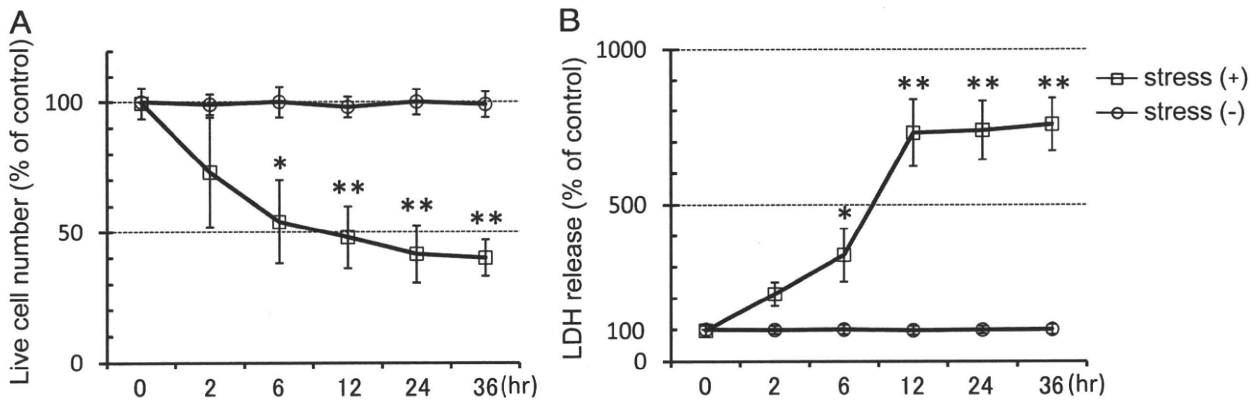

Figure 3. The survival rate (%) of living cells (**A**) and the rate of LDH release (%,**B**) after stress application. Survival rate (**A**) and LDH release (**B**) of spinal cord cells under stress-free condition (control) and tensile stress. Data are expressed as mean ± SEM (n = 6). *P < 0.05 and **P < 0.01, compared with baseline (0 hour).

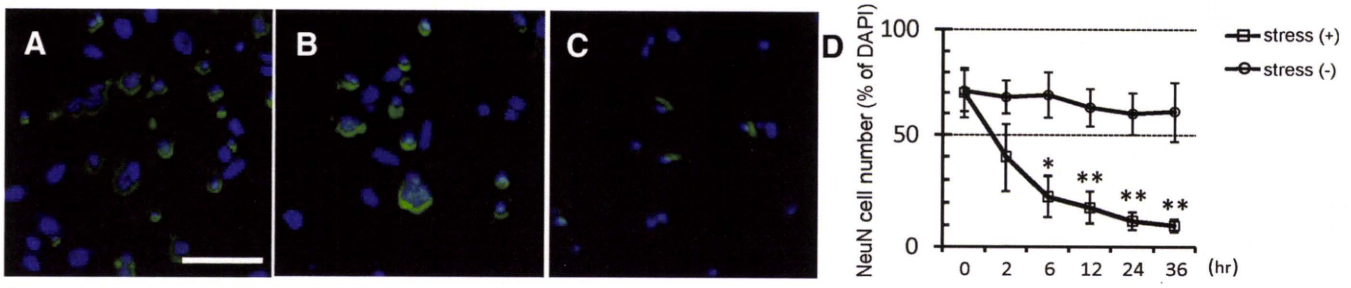

Figure 4. Number of DAPI-(blue) and NeuN-labeled cells (green) at 0 hour (**A**), 6 hours (**B**), and 24 hours (**C**) decreased with time under cyclic tensile stress. NeuN-labeled cells were more abundant than DAPI-labeled cells. **D**, The ratio of the number of DAPI-labeled cells to that of NeuN-labeled cells decreased gradually and significantly. Bar = 100 μm. Values are expressed as mean ± SEM (n = 6). $*P < 0.05$ and $**P < 0.01$, compared to nonstress cells at each time.

Effects of Cyclic Tensile Stress on mRNA Expression Levels

Time-dependent changes in mRNA expression levels of NGF, BDNF, NT-3, NT-4/5, trkA, trkB, trkC, $p75^{NTR}$, GDNF, GFRα-1, caspase-3, and caspase-9 were examined in neuronal-rich cultures subjected to mechanical stress (Figure 5). The mRNA expression levels of NGF, BDNF, and GDNF significantly increased at an early period of mechanical stress, whereas NT-3 and NT-4/5 mRNA levels remained the same throughout the application of the cyclical force. NGF and GDNF mRNA levels started to increase 2 hours after the application of stress, reached peak levels at 6 or 12 hours, and gradually decreased until 36 hours. However, changes in BDNF mRNA level were relatively small, though significant; *i.e.*, an increase was detected first at 6 hours and persisted until 24 hours after mechanical stress. The mRNA expression levels of trkB and $p75^{NTR}$, but not those of trkA, trkC, and GFR-α1, were significantly upregulated, compared to the control. The $p75^{NTR}$ mRNA level started to rise somewhat later, 6 hours after stress application, attained maximum level at 12 hours after stress, and gradually decreased until 36 hours. The mRNA expression level of caspase-9 significantly increased at 2 or 6 hours and decreased gradually until 24 hours, whereas that of caspase-3 increased in the early period after stimulation but then decreased subsequently and no difference with the control was noted at later time intervals.

Effects of Cyclic Tensile Stress on NGF, BDNF, $p75^{NTR}$, and GDNF Expression in Spinal Cord Neurons

Although the number of NeuN-labeled cells decreased gradually in a time-dependent manner, NGF, BDNF, $p75^{NTR}$, and GDNF immunoreactivities increased soon after the application of tensile stress on primary spinal cord cells. Immunoreactivities to NGF, BDNF, $p75^{NTR}$, and GDNF were increased at 6 hours under cyclic tensile stress and colocalized with the majority of the diminishing NeuN-positive cells (Figure 6). These results demonstrate that surviving neurons subjected to mechanical stress synthesized some NTs and their receptors.

■ Discussion

Several researchers have used *in vitro* models of mechanical trauma to the central nervous system, but studies on neuronal cells seems to be limited to the usage of immortalized cell lines, such as NG108–15[27,28] and PC12.[29,30] These studies indicated that mechanical stretch disrupted ionic homeostasis,[27] increased cell membrane permeability,[29] and disrupted membrane integrity, followed by neuronal loss or release of LDH. Pfister *et al*[28] used glioma cell line and reported that stretch injury resulted in overexpression of Bcl-2 family (NG108–15) followed by neuronal cell death. However, the use of neuronal cell lines as an *in vitro* injury model has at least 1 major disadvantage. Although some are derived from neuronal cells, these cell lines consist of immortalized or cancerous cells with the ability to divide uncontrollably, suggesting that their pattern of gene and/or protein expression may be significantly different from the finally differentiated, functioning neurons. Hence, although limited to the immature or developing spinal cord, we used primary cultured cells, and the method requires no treatment and retains the biomechanical and molecular fidelity of spinal cord cells *in vivo*.

Previous studies showed that subjecting the cells to relatively high nonphysiologic strain induced axonal injury and neuronal cell death.[27–29] The effects of physiologic strain on neuronal cells also varied probably due to the use of different equipments. However, recent studies examining the effect of *in vitro* mechanical stress on neuronal cells indicated that mild neurotrauma induces secondary mechanisms that ultimately lead to differentiation of neurons in mixed cortical cultures,[31] and that the effect of microtexture on neurite outgrowth is more prominent under low than high mechanical stress.[32] Based on the previous *in vivo* studies on spinal cord tensile stress,[5,6] we selected the tensile stress most appropriate to our culture system in a series of preliminary experiments. However, our results showed morphologic changes of vacuole formation within the cell soma and shrinkage of neurite arborization and release of LDH during the time course of tensile stress application. Unexpectedly, our results also indicated a decrease in neu-

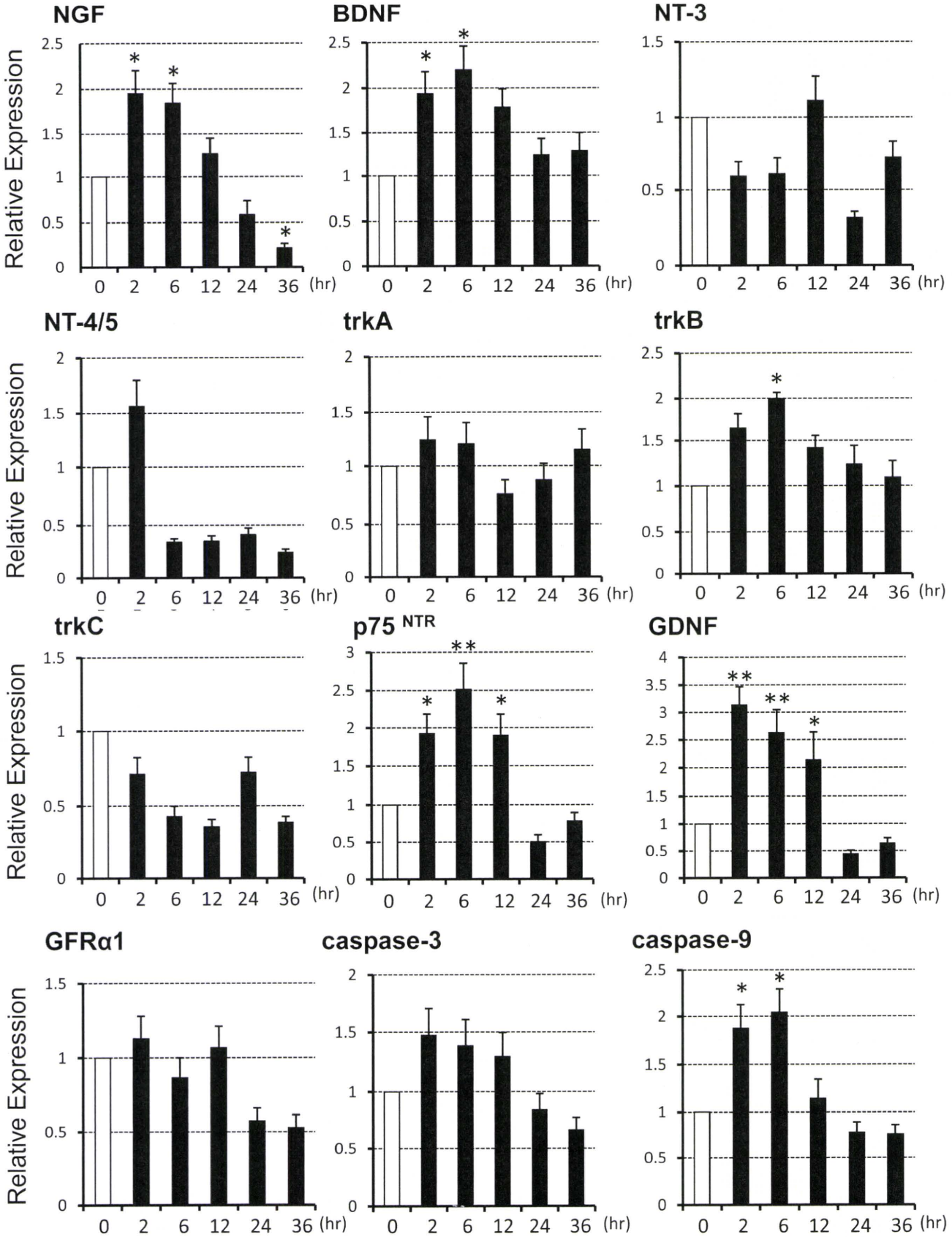

Figure 5. Effects of cyclic tensile stress on mRNA expression levels using transcription polymerase chain reaction. There were significant increases in mRNA expression levels of NGF, BDNF, trkB, p75 ^{NTR}, GDNF, and caspase-9 at early time period after application of tensile stress. Data are mean ± SEM (n = 3). $*P < 0.05$ and $**P < 0.01$.

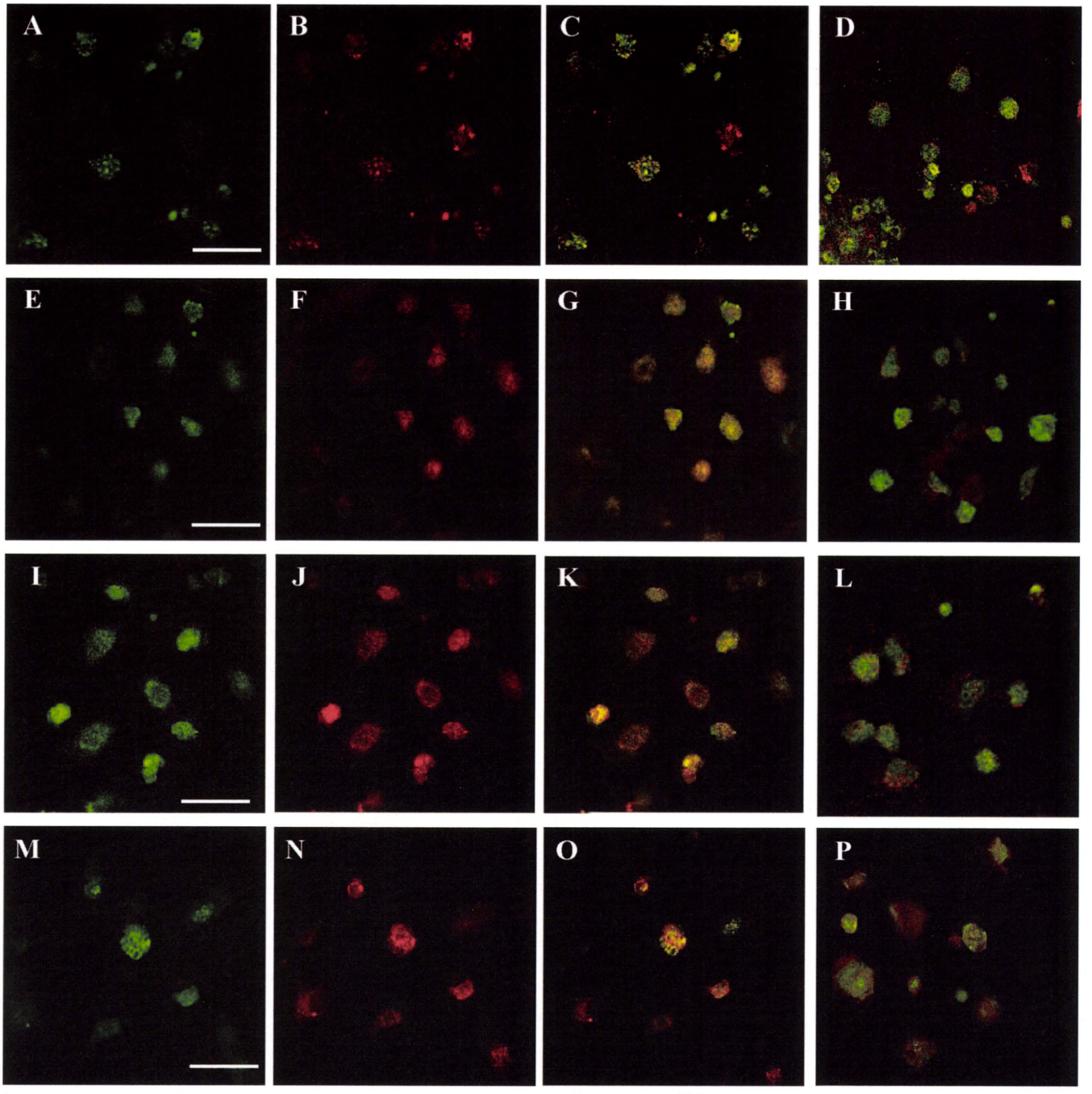

Figure 6. Confocal laser scanning microscopy showing expression of NGF, BDNF, $p75^{NTR}$, and GDNF in spinal cord neurons under cyclic tensile stress. At 6 hours after stress application, NeuN-positive cells were visualized with Alexa 488-conjugated antimouse IgG (**A, E, I, M**), NGF (**B**), BDNF (**F**), $p75^{NTR}$ (**J**), or GDNF (**N**) then with Alexa 594-conjugated antirabbit IgG. **A** and **B** are merged in **C, E,** and **F** in **G, I,** and **J,** in **K,** and **M,** and **N,** in **O**. Merged photographs for the absence of tensile stress (control) or 0 hour are shown between NGF (**D**), BDNF (**H**), $p75^{NTR}$ (**L**) or GDNF (**P**) and NeuN. Overlap in expression of NeuN protein and neurotrophic factors and receptor is shown in yellow. Bar = 100 μm.

ronal survival rate from 71% at 0 hour to 12% at 36 hours, even under lower physiologic mechanical condition. In primary cultures, isolated neurons may be more susceptible to mechanical damage than astrocytes or other cells.[17] Further studies are warranted on the condition of culture cells (time, concentration, and others) and material coating of the well bottom during stretch injury necessary to maintain a higher survival rate of spinal cord neurons.

NTs are required for neuronal survival and influence neurite elongation during development.[33] The expression of NGF family (NGF, BDNF, NT-3, and NT-4/5) and their receptors (trkA, trkB, and trkC) under mechanical compression may be essential for maintaining cell survival mechanism and prevention of cell death. We have been also interested in understanding the capacity of mechanically injured spinal cord to restore its function.[3,4,13,14,34–36] In the present study, NGF, BDNF, and

trkB mRNA expression levels increased significantly at an early time period after application of tensile stress, but NT-3, NT-4/5, trkA, and trkC mRNA levels showed no significant elevation throughout the experiment. Expression of NGF, BDNF, and trkB genes is dependent on neuronal activity, and changes in intracellular Ca^{2+} homeostasis activate these signaling pathways.[37,38] Disruption of intracellular Ca^{2+} homeostasis after mechanical tensile stress[27] may induce overexpression of NGF, BDNF, and trkB mRNAs for survival and prevention of cell death. Our results showed that NGF and GDNF gene expression levels were similar to those reported previously.[15,39] Although it has been shown that GDNF is a neurotrophic factor for motoneurons and central nervous system neurons,[40,41] it is also expressed in glial cells especially in activated microglia/macrophages of injured neural tissue.[42] Although neuronal-rich culture cells (71% of NeuN-positive cells) were used in our experiment, other cells including glial cells, with the exception of neurons, could affect our results because this culture contained a heterogeneous cell population. NT-3 is also known to play a role in neurite elongation,[13,34] thus in the present study, cultured neuronal cells required NGF, BDNF, and GDNF but not NT-3 or, presumably, NT-4/5 peptides.

Apoptotic and necrotic cell death after mechanical injury occurs through several and different pathways in neuronal tissue. The $p75^{NTR}$ is a NT receptor that can bind to all NTs at equal affinity in most cells, but it binds with a higher affinity to the proform NGF in neurons.[43] Although the function of $p75^{NTR}$ remains elusive, it is known to promote cell survival either in association with tyrosine kinase receptors or by itself.[44] Paradoxically, its activation has also been shown to promote apoptotic cell death in neurons and oligodendrocytes, and $p75^{NTR}$-induced cell death follows the intrinsic apoptotic death pathway with release of cytochrome C from the mitochondria and activation of caspase-9.[45] Our preliminary results on $p75^{NTR}$ and caspase-9 gene expression profiles are in agreement with these reports. On the other hand, caspase-3 increased after stimulation but the difference from the control was not significant. One possible explanation for this finding is that because caspase-3 is activated by both the intrinsic and extrinsic pathways, it is possible that upregulation of the intrinsic pathway may reduce apoptosis through the extrinsic pathway. Further studies are warranted to examine the roles of $p75^{NTR}$ and caspase mRNAs or proteins in the apoptotic pathways activated by tensile stress in the spinal cord. At this stage, however, there is virtually no information on the roles of $p75^{NTR}$ in spinal cord cells under tensile stress.

What is the clinical significance of our findings? The present results may help enhance our understanding of cervical myelopathy in patients with severe kyphotic flexion deformity and those with film terminale and tethered cord syndrome, or even acute central spinal cord injury (particularly Schneider type I and II). The results also suggest that treatment with certain neurotrophic factors and receptors could promote the survival of spinal cord neuronal and glial cells and rescue them against apoptosis, even under repetitive and injurious tensile stress. These results add further support to recent studies in animals treated with viral vectors carrying NTs[34–36] and suggest that such treatment could be potentially useful clinically in patients with spinal cord cells damaged by distraction injuries and even in decompressive surgery for patients with spinal cord tensile stress.

In conclusion, our results suggest that spinal cord neuronal cells survive by increasing the synthesis and utilization of several neurotrophic factors and their receptors under injurious tensile stress. Changes in the expression of these genes at an early period after mechanical stress suggest the readiness of spinal cord neurons to undergo apoptosis or necrosis. A close examination of the effects of mechanical stress on spinal cord cells *in vitro* may be the key to elucidating the adaptation of spinal cord to mechanical tensile stress.

■ Key Points

- We investigated the *in vitro* effects of cyclic tensile stress on cultured spinal cord cells, especially the expressions of neurotrophins and their receptor genes.
- Upregulation of NGF, BDNF, trkB, $p75^{NTR}$, GDNF, and caspase-9 was evident at 6 hours after application of tensile stress.
- Cyclic tensile stress increased mRNA expression and immunoreactivities of several neurotrophic factors and their receptors and induced morphologically confirmed necrotic cell death and increase in LDH release.

References

1. Hung TK, Chang GL. Biomechanical and neurological response of the spinal cord of a puppy to uniaxial tension. *J Biomech Eng* 1981;103:43–7.
2. Margulies SS, Meaney DF, Bilston LB, et al. In vivo motion of the human cervical spinal cord in extension and flexion. In: Proceedings of the 1992 IRCOBI Conference. Verona, Italy.
3. Baba H, Maezawa Y, Imura S, et al. Quantitative analysis of the spinal cord motoneuron under chronic compression: an experimental observation in the mouse. *J Neurol* 1996;243:109–16.
4. Baba H, Maezawa Y, Uchida K, et al. Three-dimensional topographic analysis of spinal accessory motoneurons under chronic mechanical compression: an experimental study in the mouse. *J Neurol* 1997;244:222–9.
5. Panjabi MM, White AA III. Physical properties and functional biomechanics of the spine: the spinal cord. In: White AA III, Panjabi MM, eds. *Clinical Biomechanics of the Spine*. 2nd ed. Philadelphia, PA: JB Lippincott; 1996: 67–71.
6. Kawahara N, Baba H, Nagata S, et al. Experimental studies on the spinal cord evoked potentials in cervical spine distraction injuries. In: Shimoji K, Kurokawa T, Tamaki T, et al, eds. *Spinal Cord Monitoring and Electrodiagnosis*. Tokyo, Japan: Springer-Verlag; 1991:107–15.
7. Bilston LE, Thibault LE. The mechanical properties of the human cervical spinal cord in vitro. *Ann Biomed Eng* 1996;24:67–74.
8. Shimizu K, Nakamura M, Nishikawa Y, et al. Spinal kyphosis causes demyelination and neuronal loss in the spinal cord: a new model of kyphotic deformity using juvenile Japanese small game fowls. *Spine* 2005;30: 2388–92.
9. Dougherty KD, Dreyfus CF, Black IB. Brain-derived neurotrophic factor in astrocytes, oligodendrocytes, and microglia/macrophages after spinal cord injury. *Neurobiol Dis* 2000;7:574–85.

10. Hayashi M, Ueyama T, Nemoto K, et al. Sequential mRNA expression for immediate early genes, cytokines, and neurotrophins in spinal cord injury. *J Neurotrauma* 2000;17:203–18.
11. Houle JD, Ye JH. Survival of chronically-injured neurons can be prolonged by treatment with neurotrophic factors. *Neuroscience* 1999;94:929–36.
12. Ikeda O, Murakami M, Ino H, et al. Acute up-regulation of brain-derived neurotrophic factor expression resulting from experimentally induced injury in the rat spinal cord. *Acta Neuropathol* 2001;102:239–45.
13. Uchida K, Baba H, Maezawa Y, et al. Histological investigation of spinal cord lesions in the spinal hyperostotic mouse (twy/twy): morphological changes in anterior horn cells and immunoreactivity to neurotrophic factors. *J Neurol* 1998;245:781–93.
14. Uchida K, Baba H, Furukawa S, et al. Increased expression of neurotrophins and their receptors in the mechanically compressed spinal cord of the spinal hyperostotic mouse (twy/twy). *Acta Neuropathol* 2003;106:29–36.
15. Widenfalk J, Lundströmer K, Jubran M, et al. Neurotrophic factors and receptors in the immature and adult spinal cord after mechanical injury or kainic acid. *J Neurosci* 2001;21:3457–75.
16. Popovich PG, Strokes BT, Whitacre CC. Concept of autoimmunity following spinal cord injury: possible roles for T lymphocytes in the traumatized central nerve system. *J Neurosci Res* 1996;45:349–63.
17. Morrison B III, Saatman KE, Meaney DF, et al. In vitro central nervous system models of mechanically induced trauma. A review. *J Neurotrauma* 1998;15:911–28.
18. Gilbert JA, Weinhold PS, Banes AJ, et al. Strain profiles for circular cell culture plates containing flexible surfaces employed to mechanically deform cells in vitro. *J Biomech* 1994;27:1169–77.
19. Matsumoto T, Kawakami M, Kuribayashi K, et al. Cyclic mechanical stretch stress increases the growth rate and collagen synthesis of nucleus pulposus cells in vitro. *Spine* 1999;24:315–9.
20. Nakatani T, Marui T, Hirota T, et al. Mechanical stretching force promotes collagen synthesis by cultured cells from human ligamentum flavum via transforming growth factor-β1. *J Orthop Res* 2002;20:1380–6.
21. Arakawa Y, Sendtner M, Thoenen H. Survival effect of ciliary neurotrophic factor (CNTF) on chick embryonic motoneurons in culture: comparison with other neurotrophic factors and cytokines. *J Neurosci* 1990;10:3507–15.
22. Demestre M, Pullen A, Orrell RW, et al. ALS-IgG-induced selective motor neuron apoptosis in rat mixed primary spinal cord cultures. *J Neurochem* 2005;94:268–75.
23. Vaughan PJ, Pike CJ, Cotman CW, et al. Thrombin receptor activation protects neurons and astrocytes from cell death produced by environmental insults. *J Neurosci* 1995;15:5389–401.
24. Takeno K, Kobayashi S, Negoro K, et al. Physical limitations to tissue engineering of intervertebral disc cells: effect of extracellular osmotic change on glycosaminoglycan production and cell metabolism. Laboratory investigation. *J Neurosurg Spine* 2007;7:637–44.
25. McInnis J, Wang C, Anastasio N, et al. The role of superoxide and nuclear factor-κB signaling in N-methyl-D-aspart-induced necrosis and apoptosis. *J Pharmacol Exp Ther* 2002;301:478–87.
26. Liao PC, Lieu CH. Cell cycle specific induction of apoptosis and necrosis by paclitaxel in the leukemic U937 cells. *Life Sci* 2005;76:623–39.
27. Cargill RS, Thibauble LE. Acute alterations in [Ca^{2+}]in NG108–15 cells subjected to high strain rate deformation and chemical hypoxia: an in vitro model for neural trauma. *J Neurotrauma* 1996;13:396–407.
28. Pfister B, Oyler G, Betenbaugh M, et al. The effect of bclX$_L$ Bax overexpression on stretch-injury induced neural cell death. *Mech Chem Biosyst* 2004;1:233–43.
29. Geddes DM, Cargill RS, Laplace MC. Mechanical stretch to neurons results in a strain rate and magnitude-dependent increase in plasma membrane permeability. *J Neurotrauma* 2003;20:1039–49.
30. Serbest G, Horwitz J, Barbee K. The effect of poloxamer-188 on neuronal cell recovery from mechanical injury. *J Neurotrauma* 2005;22:119–32.
31. Arundine M, Aarts M, Lau A, et al. Vulnerability of central neurons to secondary insults after in vitro mechanical stretch. *J Neurosci* 2004;24:8106–23.
32. Haq F, Keith C, Zhang G. Neurite development in PC12 cells on flexible micro-textured substrates under cyclic stretch. *Biotechnol Prog* 2006;22:133–40.
33. Bregman BS. Transplants and neurotrophins modify the response of developing and mature CNS neurons to spinal cord injury. Axonal regeneration and recovery of function. In: Kalb RG, Strittmatter SM, eds. *Neurobiology of Spinal Cord Injury*. Totowa, NJ: Humana Press; 2000:169–94.
34. Uchida K, Nakajima H, Inukai T, et al. Retrograde transfection of adenovirus vector carrying neurotrophin-3 gene enhances survival of anterior horn neurons of twy/twy mice with chronic mechanical compression of the spinal cord. *J Neurosci Res* 2008;86:1789–800.
35. Nakajima H, Uchida K, Kobayashi S, et al. Rescue of anterior horn neurons after spinal cord injury by retrograde transfection of adenovirus vector carrying brain-derived neurotrophic factor gene. *J Neurotrauma* 2007;24:703–12.
36. Xu K, Uchida K, Nakajima H, et al. Targeted retrograde transfection of adenovirus vector carrying brain-derived neurotrophic factor gene prevents loss of mouse (twy/twy) anterior horn neurons in vivo sustaining mechanical compression. *Spine* 2006;31:1867–74.
37. Poulsen FR, Lauterborn J, Zimmer J, et al. Differential expression of brain-derived neurotrophic factor transcripts after pilocarpine-induced seizure-like activity is related to mode of Ca2+ entry. *Neuroscience* 2004;126:665–76.
38. Zafra F, Hengerer B, Leibrock J, et al. Activity dependent regulation of BDNF and NGF mRNAs in the rat hippocampus is mediated by non-NMDA glutamate receptors. *EMBO J* 1990;9:3545–50.
39. Murakami Y, Furukawa S, Nitta A, et al. Accumulation of nerve growth factor protein at both rostral and caudal stumps in the transected rat spinal cord. *J Neurol Sci* 2002;198:63–9.
40. Lin LF, Shin K, Bao P, et al. GDNF: a glial cell line-derived neurotrophic factor for midbrain dopaminergic neurons. *Science* 1993;260:1130–2.
41. Henderson CE, Phillip HS, Pollock RA, et al. GDNF: a potent survival factor for motoneurons present in peripheral nerve and muscle. *Science* 1994;266:1062–4.
42. Hashimoto M, Nitta A, Fukumitsu H, et al. Involvement of glial cell line-derived neurotrophic factor in activation processes of rodent macrophages. *J Neurosci Res* 2005;79:476–87.
43. Lee R, Kermani P, Teng KK, et al. Regulation of cell survival by secreted proneurotrophin. *Science* 2001;294:1945–8.
44. Baker PA. p75NTR: a study in contrasts. *Cell Death Differ* 1998;5:346–56.
45. Bhakar AL, Howell JL, Paul CE, et al. Apoptosis induced by $p75^{NTR}$ overexpression requires Jun kinase-dependent phosphorylation of bad. *J Neurosci* 2003;11373–81.

J Neurosurg Spine 9:600–610, 2008

Reduction of cystic cavity, promotion of axonal regeneration and sparing, and functional recovery with transplanted bone marrow stromal cell–derived Schwann cells after contusion injury to the adult rat spinal cord

Laboratory investigation

Yukio Someya, M.D.,[1] Masao Koda, M.D., Ph.D.,[3] Mari Dezawa, M.D., Ph.D.,[4] Tomoko Kadota, M.D., Ph.D.,[2] Masayuki Hashimoto, M.D., Ph.D.,[3] Takahito Kamada, M.D., Ph.D.,[1] Yutaka Nishio, M.D., Ph.D.,[1] Ryo Kadota, M.D., Ph.D.,[1] Chikato Mannoji, M.D., Ph.D.,[1] Tomohiro Miyashita, M.D., Ph.D.,[1] Akihiko Okawa, M.D., Ph.D.,[1] Katsunori Yoshinaga, M.D., Ph.D.,[5] and Masashi Yamazaki, M.D., Ph.D.[1]

Departments of [1]Orthopaedic Surgery and [2]Bioenvironmental Medicine, Chiba University Graduate School of Medicine, Chiba; [3]Department of Orthopaedic Surgery, Prefectural Togane Hospital, Chiba; [4]Department of Anatomy and Neurobiology, Kyoto University Graduate School of Medicine, Kyoto; and [5]Chiba Rehabilitation Center, Chiba, Japan

Object. The authors previously reported that Schwann cells (SCs) could be derived from bone marrow stromal cells (BMSCs) in vitro and that they promoted axonal regeneration of completely transected rat spinal cords in vivo. The aim of the present study is to evaluate the efficacy of transplanted BMSC-derived SCs (BMSC-SCs) in a rat model of spinal cord contusion, which is relevant to clinical spinal cord injury.

Methods. Bone marrow stromal cells were cultured as plastic-adherent cells from the bone marrow of GFP-transgenic rats. The BMSC-SCs were derived from BMSCs in vitro with sequential treatment using beta-mercaptoethanol, all-*trans*-retinoic acid, forskolin, basic fibroblast growth factor, platelet derived–growth factor, and heregulin. Schwann cells were cultured from the sciatic nerve of neonatal, GFP-transgenic rats. Immunocytochemical analysis and the reverse transcriptase–polymerase chain reaction were performed to characterize the BMSC-SCs. For transplantation, contusions with the New York University impactor were delivered at T-9 in 10- to 11-week-old male Wistar rats. Four groups of rats received injections at the injury site 7 days postinjury: the first received BMSC-SCs and matrigel, a second received peripheral SCs and matrigel, a third group received BMSCs and matrigel, and a fourth group received matrigel alone. Histological and immunohistochemical studies, electron microscopy, and functional assessments were performed to evaluate the therapeutic effects of BMSC-SC transplantation.

Results. Immunohistochemical analysis and reverse transcriptase–polymerase chain reaction revealed that BMSC-SCs have characteristics similar to SCs not only in their morphological characteristics but also in their immunocytochemical phenotype and genotype. Histological examination revealed that the area of the cystic cavity was significantly reduced in the BMSC-SC and SC groups compared with the control rats. Immunohistochemical analysis showed that transplanted BMSCs, BMSC-SCs, and SCs all maintained their original phenotypes. The BMSC-SC and SC groups had a larger number of tyrosine hydroxilase–positive fibers than the control group, and the BMSC-SC group had more serotonin-positive fibers than the BMSC or control group. The BMSC-SC group showed significantly better hindlimb functional recovery than in the BMSC and control group. Electron microscopy revealed that transplanted BMSC-SCs existed in association with the host axons.

Conclusions. Based on their findings, the authors concluded that BMSC-SC transplantation reduces the size of the cystic cavity, promotes axonal regeneration and sparing, results in hindlimb functional recovery, and can be a useful tool for spinal cord injury as a substitute for SCs. *(DOI: 10.3171/SPI.2008.9.08135)*

Key Words • bone marrow stromal cell • cell transplantation • hindlimb function • Schwann cell • spinal cord injury

It has been widely believed that a lesioned adult mammalian spinal cord cannot regenerate. Recent advances in stem cell research have enabled us to repair injured spinal cords by means of various kinds of cell therapies, including the use of embryonic stem cells,[33] fetal neural stem cells,[36] and adult neural stem cells.[15] Major obstacles to the use of these cells in clinical trials

Abbreviations used in this paper: ANOVA = analysis of variance; BBB = Basso, Beattie, Bresnahan; BDA = biotinylated dextrin amine; BMSC = bone marrow stromal cell; BMSC-SC = BMSC-derived Schwann cell; FBS = fetal bovine serum; HSC = hematopoietic stem cell; MEM = minimum essential medium; PBS = phosphate-buffered saline; RT-PCR = reverse transcriptase–polymerase chain reaction; SC = Schwann cell; SCI = spinal cord injury; SEM = standard error of the mean.

include the possibility of allograft rejection and the ethical problems raised by the use of fetal tissue; autologous transplantation may resolve these problems.

Adult bone marrow contains several different stem cell populations including HSCs and BMSCs, also called mesenchymal stem cells. Both HSCs and BMSCs are candidates for use in cell therapy for neurological disorders because they can be transplanted autologously. Indeed, it has been reported that bone marrow cells have the potential to restore injured spinal cord tissue and promote functional recovery. In fact, transplantation of HSCs promotes functional recovery after compression-induced SCI in mice[28,29] and transplantation of BMSCs significantly improves hindlimb function after SCI in mice and rats.[12,24,37,49] However, the therapeutic efficacy of BMSCs for SCI is still controversial. Several researchers have suggested that BMSC transplantation cannot promote functional recovery.[1,53] In addition, transplantation of the non–neural lineage cells has potential problems including differentiation of transplanted cells and compatibility with the host spinal cord. Differentiation into neural lineage cells prior to transplantation could enhance the therapeutic effect of BMSCs and offer a solution to these problems.

We recently reported that cells with SC properties could be derived from BMSCs in vitro, and that they effectively promoted regeneration of lesioned sciatic nerves.[17,34] Moreover, we have previously reported that transplantation of BMSC-SCs effectively promotes regeneration of damaged axons and hindlimb functional recovery in completely transacted adult rat spinal cord.[27]

The aim of the present study is to evaluate the therapeutic effects of BMSC-SC transplantation in adult rats with contusive SCIs, a more clinically relevant model than the spinal cord transection model. Additionally, we compared BMSC-SC transplantation with transplantation of untreated BMSCs and peripheral nerve–derived SCs, which are widely known to promote recovery of the injured spinal cord and aid in tissue restoration, survival of transplanted cells, axonal regeneration/sparing, and promotion of hindlimb functional recovery.

Methods

Cell Cultures and In Vitro Differentiation

Bone marrow stromal cells were cultured as previously described.[27] Briefly, total bone marrow cells were collected from the femurs of adult male GFP-transgenic Wistar rats (provided by the YS Institute, Inc.) and plated onto plastic culture dishes. The cells adherent to the dishes were cultured as BMSCs in alpha-MEM (Sigma) supplemented with 20% FBS. The BMSCs were used for transplantation and in vitro induction experiments between passages 4 to 6.

Peripheral SCs were cultured from dissected sciatic nerves of 2-day-old GFP-transgenic Wistar rats.[21,32] The dissected nerves were treated with 0.1% collagenase and 0.1% trypsin in PBS for 60 minutes at 37°C. Dissociated cells were cultured in Dulbecco modified Eagle medium containing 10% FBS and 1% antibiotics (100 U/ml penicillin and 100 μg/ml streptomycin). After 1 day of culturing, cells were exposed to 2 cycles of cytosine-arabinoside treatment (10 μM) for 3 days to prevent proliferation of fibroblasts. After 7 days of culturing, cells were plated on dishes coated with poly-L-lysine (Sigma) in Dulbecco modified Eagle medium containing 10% FBS, 1% antibiotics, and 10-μM forskolin (Sigma). Cells were maintained in a 37°C incubator containing 5% CO_2 and passaged when confluent. The medium was changed every 3 days. Bone marrow stromal cells were derived from SCs in vitro as previously described.[17,27] Briefly, the BMSCs were incubated with alpha-MEM containing 1-mM beta-mercaptoethanol for 24 hours. After washing the cells, the medium was replaced with alpha-MEM containing 10% FBS and 35 ng/ml all-transretinoic acid (Sigma) for 3 days. Cells were then transferred to alpha-MEM containing 10% FBS, 5-μM forskolin (Calbiochem), 10 ng/ml recombinant human basic fibroblast growth factor (Peprotech), 5 ng/ml platelet derived growth factor (Peprotech), and 200 ng/ml heregulin β1 (R&D Systems) for 7 days.

Immunohistochemical analysis was performed to characterize the BMSC-SCs in vitro. Mouse monoclonal anti-vimentin antibody (1:200; Dako Cytomation) and mouse monoclonal anti-fibronectin antibody (1:400; Chemicon International) were used as markers for BMSCs. Mouse monoclonal anti–protein zero antibody (P0, 1:300; Astexx), rabbit polyclonal anti-S100 antibody (1:100; Dako Cytomation), and rabbit polyclonal anti-p75NTR antibody (1:200; Chemicon) were used as markers for SCs. Cell nuclei were stained with 4'-6-diamidino-2-phenylindole (Molecular Probes). A negative control was performed by omitting the primary antibodies.

The RT-PCR Analysis

Total RNA from the cells was extracted with TRIzol Reagent (Invitrogen) and purified according to the manufacturer's instruction. From 5 μg of RNA, the first cDNA strand was generated using SuperScript II-RT (Invitrogen). The PCR reactions were performed using Ex Taq DNA polymerase (TaKaRa). The conditions for amplification were as follows: 30 seconds at 94°C, 30 seconds at 60°C, and 30 seconds at 72°C for 30 cycles (25 cycles for beta-actin) and the final incubation at 72°C for an additional 4 minutes. We used the following primers specific to SC genes, designed by Primer3 software, and beta-actin was used as internal control. The Krox20 (Egr2) sense strand was 5'-CAGGAGTGACGAAAGGAAGC-3' and the antisense was 5'-ATCTCACGGTGTCCTGGTTC-3'; Krox24 (Egr1), sense: 5'-GACGAGTTATCCCAGCCAAA-3' and antisense: 5'-AGGCAGAGGAAGACGATGAA-3'; P0, sense: 5'-GATGGGCAGTCTGCAGTGTA -3' and antisense: 5'-TTTGGCAGGTGTCAAGTGAG -3'; beta-actin, sense: 5'-TAAAGACCTCTATGCCAACAC-3' and antisense: 5'-CTCCTGCTTGCTGATCCACAT-3'.

Spinal Cord Injury and Transplantation

For experimental SCI, we used 48 male Wistar rats 10–11 weeks old (weight 225–250 g) divided into 3 experimental and 1 control group of 12 animals each. A

laminectomy was performed at the T8–9 level. The moderate contusion injury was created with a New York University impactor (10-g rod and 25-mm height).[5,54] Afterwards the rats' muscles and skin were sutured in layers and they were placed in warm cages overnight; food and water were provided ad libitum. Manual bladder expression was performed twice daily until the rats recovered bladder reflexes. All animals were given antibiotic medication in their drinking water (1.0-ml bactramin in 500-ml acidified water) for 2 weeks after injury.

Seven days after injury, the injured site was reexposed and transplantation was performed. The BMSC group was injected with a mixture of matrigel and BMSCs (5×10^5/5 μl), the BMSC-SC group received BMSC-SCs and matrigel (5×10^5 cells/5 μl), the SC group received peripheral SCs and matrigel (5×10^5/5 μl), and the control group received matrigel alone (5 μl). The injections were delivered to the injured site with a glass micropipette attached to a Hamilton microsyringe.

All animals received immunosuppressive treatment with cyclosporine A (Novartis), because BMSC transplantation may cause a host immunological reaction resulting in rejection of transplanted cells.[13] Twenty-four hours before transplantation, cyclosporine A (20 mg/kg) was injected subcutaneously. After transplantation, cyclosporine A was also injected for the entire experimental period (20 mg/kg on Monday and Wednesday, and 40 mg/kg on Friday).[50] No animal showed abnormal behavior. All the experimental procedures were performed in compliance with the guidelines established by the Animal Care and Use Committee of Chiba University.

Tissue Preparation

At the end of the functional assessment period 6 weeks after injury, animals were perfused transcardially with 4% paraformaldehyde in PBS (pH 7.4) after an overdose of pentobarbital anesthesia. Three spinal cord segments (T8–10) including the injury epicenter were removed and postfixed in the same fixative overnight, stored in 20% sucrose in PBS at 4°C, and embedded in Optimal Cutting Temperature compound (Sakura Finetechnical). Sagittal cryosections (12-μm thickness) were cut using a cryostat and the sections were mounted onto poly-L-lysine–coated slides (Matsunami). Every fifth section from the central portion of the spinal cords was serially mounted. At least 4 samples from each animal, each 60-μm interval within a 240-μm width centered of the lesion site, were mounted on slides and evaluated for histochemical characteristics as described below.

Anterograde Tract Tracing

Four weeks postinjury, the cranial bone overlying the motor cortex was removed and 10% BDA was injected in 4 divided doses (1–3 mm posterior to the coronal suture and 2.5-mm lateral to the coronal suture; 2 each side, 4×1 μl aliquots) bilaterally into the motor cortex using a glass micropipette attached to a Hamilton microsyringe. Two weeks after tracer injection, animals were perfused as described, and the spinal cords were dissected for staining of labeled corticospinal axons.

Cystic Cavity Measurement

To measure the area of the cystic cavity, the sections were stained with cresyl violet, dehydrated, and sealed with Permount (Fisher Scientific). At least 4 samples, each 60-μm apart, were chosen for cavity measurements; the measurements therefore covered a 240-μm width in the central portion of spinal cord including the lesion site. We measured the area of the cystic cavity using Scion Image computer analysis software (Scion Corp.). The average cystic cavity area was compared among the 4 groups of rats.

Immunohistochemical and Electron Microscopy Studies

We performed immunohistochemical studies as previously described.[23,27] Briefly, the GFP-positive cells were counted to compare with the number of surviving transplanted cells; goat polyclonal anti-GFP antibody (1:100; SantaCruz) was used as the primary antibody. The average number of surviving GFP-positive cells in 4 samples obtained from each animal was compared among the BMSC, BMSC-SC, and SC groups. To evaluate the phenotypic changes of transplanted cells, a double immunofluorescence study for GFP and cell-specific markers were performed in the BMSC, BMSC-SC, and SC groups.

Immunohistochemical analysis for axonal markers was performed to evaluate the extent of axonal regeneration and sparing. The following primary antibodies were used to detect various types of nerve fibers: rabbit polyclonal anti-Gap43 antibody (1:400; Santa-Cruz), mouse monoclonal anti–Th antibody (1:400; Chemicon), and rabbit polyclonal anti-serotonin antibody (1:5000; Sigma). After incubation with primary antibodies, the sections were incubated with Alexa 594 dye–conjugated secondary antibodies (Molecular Probes) to detect positive signals. We used Gap43 as a general marker for regenerating/sprouting nerve fibers. Tyrosine hydroxylase–positive nerve fibers are mainly cerulospinal adrenergic, and serotonin-positive nerve fibers are mainly raphe spinal serotonergic; both fiber types contribute to motor function.[7,16,43,48] To evaluate regeneration/sparing of Gap43-, Th- or serotonin-positive nerve fibers, the number of immunoreactive fibers that traversed the lines perpendicular to the central axis of the spinal cord at rostral (5-mm rostral to the injury epicenter), epicenter, and caudal (5-mm caudal to the epicenter) levels were counted and compared between groups. For the BDA tracing study, sections were immunostained with streptavidin-conjugated Alexa 594 (1:800; Molecular Probes) and examined under laser scanning confocal microscopy. The negative control was performed by omitting the primary antibodies.

The spinal cord tissue samples from the BMSC-SC group rats were cut into 100-μm-thick sections and stained with rabbit polyclonal anti-GFP antibody (Molecular Probes). Positive signals were detected with avidin-biotin complex method using the Histofine kit (Nichirei). The positive signals were visualized with diaminobenzidine and hydrogen peroxide. The sections were then postfixed with 1% OsO_4 in PBS (pH 7.4) for 1-hour and then block-stained with 1% uranyl acetate in acetate buffer, dehydrated, and embedded in Epon 812 (Shell Chemi-

cal).[26] Ultrathin sections (90-nm thickness) were stained with lead citrate. These sections were examined with JEM 1200EX electron microscope (JEOL).

Assessment of Locomotor Activity

The hindlimb functioning of the animals in all groups was assessed with the BBB locomotor scale[4] before injury and 1 day, 3 days, and each week (for 6 weeks) after injury.

Statistical Analysis

Each statistical analysis was evaluated using multiple comparisons between groups. For histological studies, the 1-way ANOVA was used, followed by Bonferroni-Dunn post hoc test. For the locomotor scale scores, repeated-measures ANOVA, and Fisher protected least significant difference post hoc test was used. For fractional BBB scores at 8 time points, the 1-way ANOVA and Bonferroni-Dunn test was used. Statistical significance was set at $p < 0.05$ and $p < 0.01$, respectively.

Results

In Vitro Character of BMSC-SCs

Bone marrow stromal cells in primary culture show a fibroblast-like morphology, and these characteristics were kept for several passages (Fig. 1A). The BMSC-SCs were successfully derived from BMSCs and appeared short and spindle-shaped (Fig. 1B). The morphological characteristics of these cells were similar to that observed in normal peripheral SCs (Fig. 1C). The BMSCs stained positive for vimentin and fibronectin (not shown), while the BMSC-SCs were positive for P0, S100 protein, and p75NTR (Fig. 1D and E), widely known markers for SCs.

Results of RT-PCR revealed that expression level of P0—an important glycoprotein in peripheral myelination that is widely known as a specific marker for SCs—increased in BMSC-SCs[31] compared with BMSCs (Fig. 1F). There was no significant difference between BMSCs and BMSC-SCs in the expression level of Krox20 and Krox24 (Fig. 1F). These data show that BMSC-SCs have characteristics similar to SCs not only in their morphological characteristics, but also in their phenotype and genotype.

To elucidate the efficacy of BMSC-SC for tissue sparing after SCI, we measured the area of cystic cavity with cresyl violet staining 5 weeks after transplantation (Fig. 2A–D). The average area of the cystic cavity was significantly smaller in BMSC-SC and SC groups ($p < 0.01$ and $p < 0.05$, respectively) than that in control group indicating that transplantation of BMSC-SCs or peripheral SCs

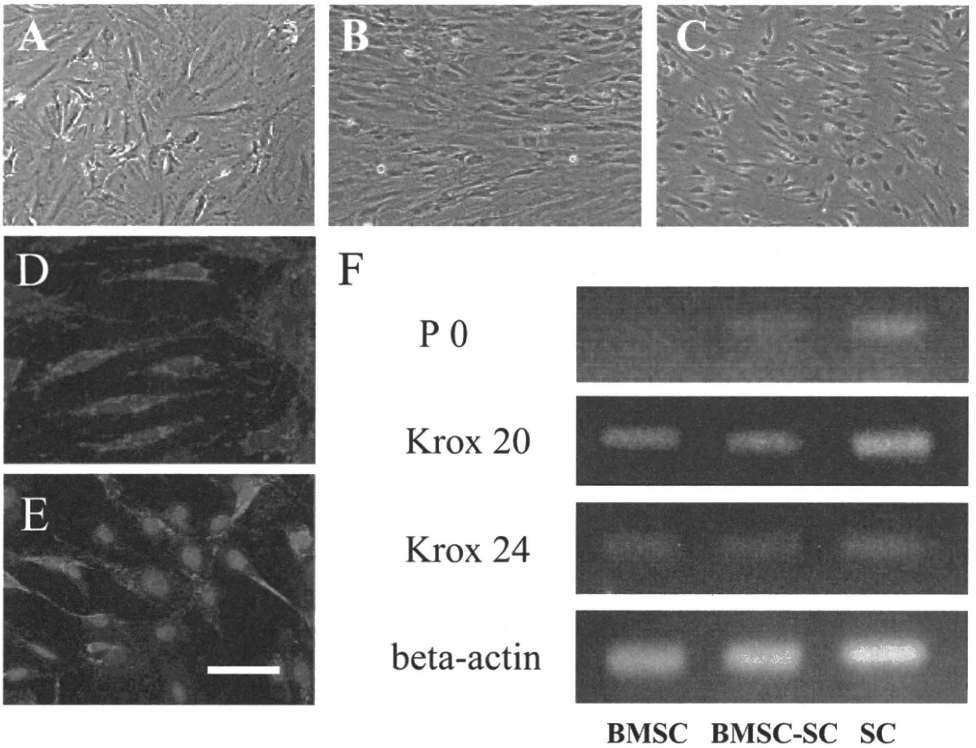

FIG. 1. Photomicrographs demonstrating the peripheral SC-like characteristics of BMSC-SCs. A: Phase-contrast microscopic image of BMSCs cultured from GFP-transgenic rats. B: Phase-contrast microscopic image of BMSC-SCs. The BMSC-SCs are morphologically and phenotypically similar to SCs. C: Phase-contrast microscopic image of peripheral SC cultured from a GFP-transgenic rat. D and E: Immunofluorescence images of BMSC-SCs stained for P0 (D) and p75NTR (E). The BMSC-SCs were positive for P0, S100, and p75NTR. Nuclei were stained with 4'-6-diamidino-2-phenylindole. Bar = 50 μm. F: Results of RT-PCR analysis showing that P0 mRNA was upregulated in BMSC-SC–like peripheral SCs. The expression level of P0 in BMSCs is shown in comparison to its expression in BMSC-SCs and SCs. No significant statistical difference was shown between BMSCs and BMSC-SCs in the expression of Krox20 and Krox24.

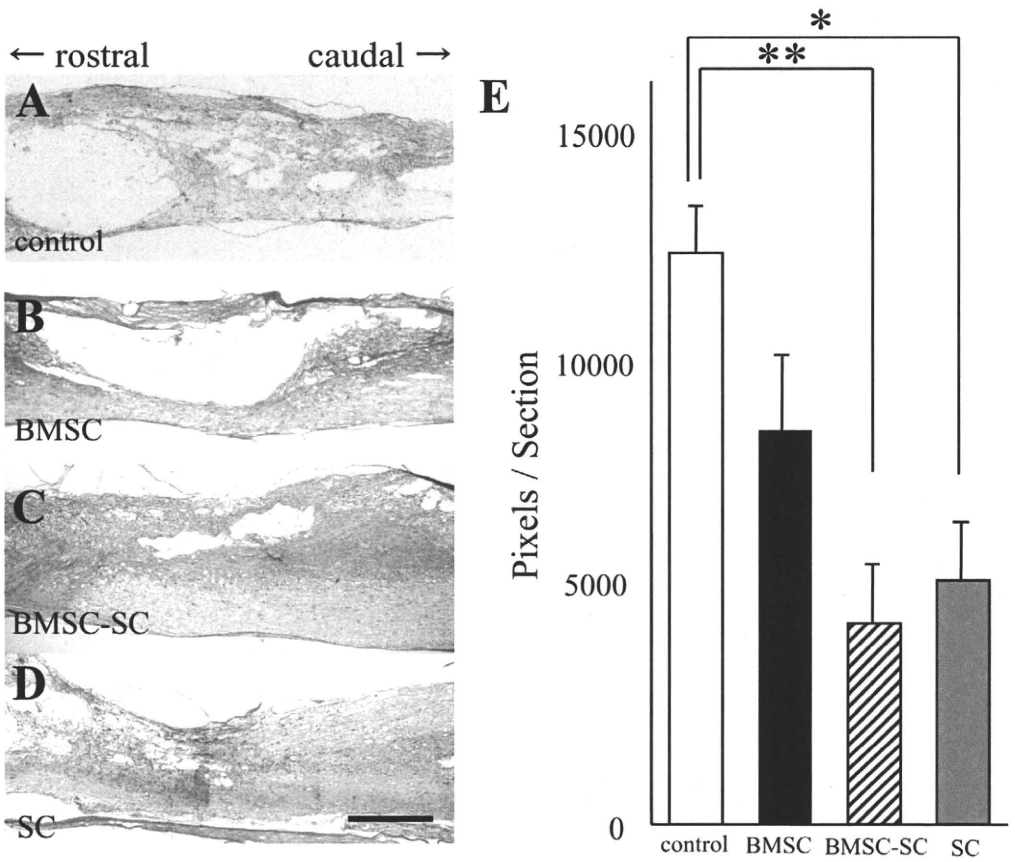

FIG. 2. A–D: Cresyl-violet–stained BMSC-SCs and SCs in preserved spinal cord tissue samples from all 4 groups. Representative image of cystic cavity in samples obtained in the control (A), BMSC (B), BMSC-SC (C), and SC (D) groups. The area of cystic cavity of BMSC-SC and SC groups were significantly smaller than that of the control group. Bar = 1 mm. E: Statistical analysis of area of cystic cavity (*white column*, control group; *black column*, BMSC group; *hatched column*, BMSC-SC group; and *gray column*, SC group). The area of cystic cavity in the BMSC-SC and SC groups was significantly smaller than that in the control group. *Bars* represent the means, and *whiskers* the SEMs. *$p < 0.05$, **$p < 0.01$.

helps to preserve spinal cord tissue (Fig. 2E). There was no significant difference in the average area of the cystic cavity between the other groups.

Phenotype of BMSC-SCs in the Injured Spinal Cord

The number of GFP-positive transplanted cells in the BMSC, BMSC-SC, and SC samples was 142.0 ± 18.0, 386.3 ± 28.6, and 1301.8 ± 310.8 per section, respectively (Fig. 3A–C). Note that the number of GFP-positive transplanted cells in the SC group was significantly larger than in the BMSC and BMSC-SC groups ($p < 0.01$; Fig. 3D). In addition, the number of GFP-positive transplanted cells in the BMSC-SC group was significantly larger than that in the BMSC group ($p < 0.05$).

A double immunofluorescence study showed that GFP-positive transplanted BMSCs were simultaneously positive for vimentin and fibronectin (data not shown). The BMSC-SCs and SCs were both positive for P0, S100, and p75NTR (not shown), indicating that the transplanted cells maintained the specific phenotypes observed in vitro even after transplantation into the injured spinal cord.

Adrenergic and Serotonergic Fibers in the Injured Spinal Cord

We next performed immunohistochemical analyses for axonal markers and anterograde axonal tracing to evaluate axonal the extent of regeneration and/or sparing. The number of Gap43-positive nerve fibers at the rostral level in the SC group was significantly larger than that in the other groups ($p < 0.01$; Figs. 4A–C and 5A). The number of Gap43-positive nerve fibers at the injury epicenter level in the BMSC-SC group (Fig. 4B) was significantly larger than that in the control ($p < 0.05$; Fig. 5A), and the number of Gap43-positive nerve fibers at the epicenter level in the SC group was significantly larger than in the control and BMSC groups ($p < 0.01$; Fig. 5A). There was no significant statistical difference in the number of Gap43-positive nerve fibers at the caudal level between the groups.

To characterize the phenotype of regenerated or spared axons, we performed immunohistochemical analysis for several nerve fiber markers. There were significantly more Th-positive fibers at the injury epicenter and caudal level in the BMSC-SC ($p < 0.01$, both locations;

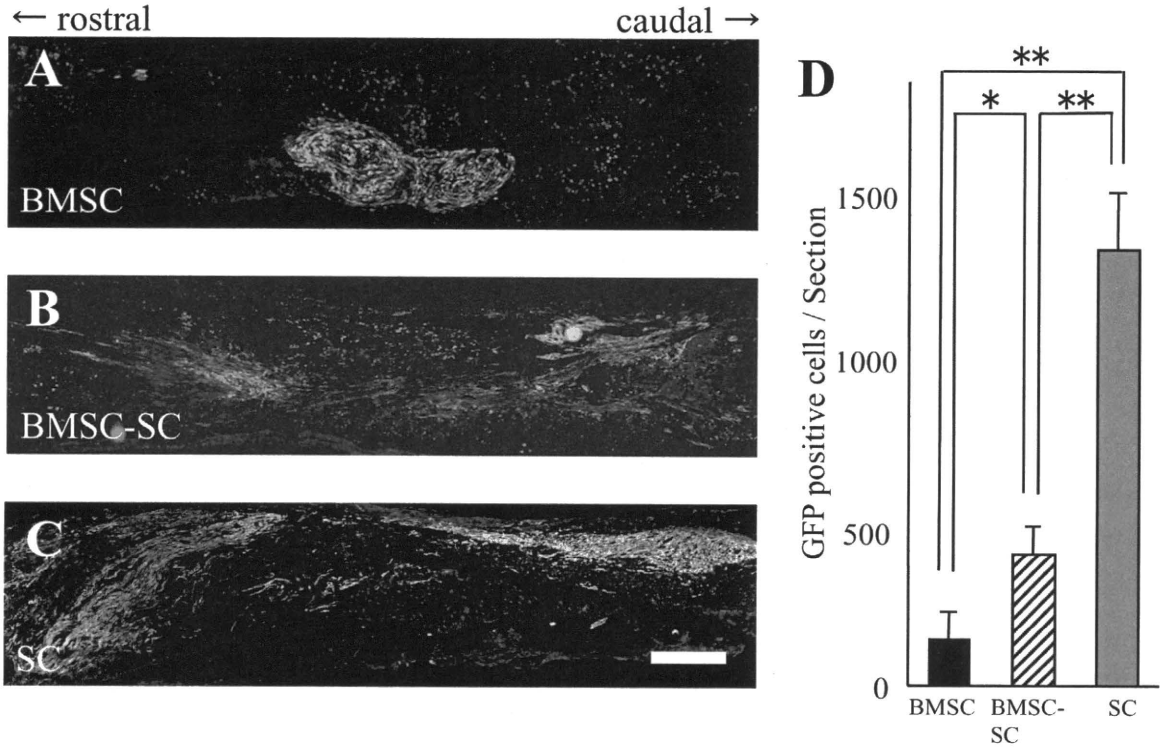

FIG. 3. Photomicrographs. Staining with GFP in the BMSC (A), BMSC-SC (B), and SC groups (C) 5 weeks after cell transplantation. Bar = 1 mm. D: Graph of the statistical analysis of number of GFP-positive transplanted cells. There were significantly more GFP-positive transplanted cells in the BMSC-SC group *(hatched column)* than in the BMSC *(black column)* group ($p < 0.05$). There were also significantly more GFP-positive transplanted cells in the SC group *(gray column)* than in the BMSC *(black column)* and BMSC-SC *(hatched column)* groups. *Bars* represent the means, and *whiskers* the SEMs. *$p < 0.05$, **$p < 0.01$.

Figs. 4D–F and 5B) and SC ($p < 0.05$ and $p < 0.01$, respectively) groups than in the control group. The number of serotonin-positive nerve fibers in the BMSC-SC group was significantly larger than that in the control and BMSC group at the caudal level ($p < 0.05$; Figs. 4I and 5C). Biotinylated dextrin amine–labeled corticospinal tract fibers were found in the rostral and epicenter levels, however there were no BDA-labeled fibers in caudal level any groups (data not shown).

In the immunoelectron microscopic study of rats from the BMSC-SC group, the GFP-positive transplanted cells (Fig. 6 *asterisks*) had several thin processes, which were immediate contact with host nerve tissues (Fig. 6 *arrows*).

Locomotor Recovery

Finally, we assessed the recovery of hindlimb functioning in all groups on a weekly basis for 6 weeks (Fig. 7). The repeated-measures ANOVA and post hoc Fisher protected least significant difference tests showed that hindlimb function recovered significantly in the BMSC-SC group compared with the control and BMSC group ($p = 0.024$ and $p = 0.047$, respectively). The average BBB recovery score in the BMSC-SC group 5 weeks after transplantation was 10.3 ± 0.8, indicating occasional weight-supported plantar steps without forelimb–hindlimb coordination, and in the BMSC group was 7.9 ± 0.6, indicating that all 3 joints of hindlimbs showed extensive movement. Five weeks after transplantation, the average recovery score 5 weeks after transplantation was 7.7 ± 0.6 in the control group, and 9.2 ± 0.8 in the SC group, indicating occasional plantar placement of the paws with weight support. Comparison among the groups at each time point revealed a statistically significant difference between the BMSC-SC and control and the BMSC-SC and BMSC groups in average BBB scores 3–5 weeks after transplantation (Fig. 7).

Discussion

In the present study, we derived SCs from BMSCs and confirmed that BMSC-SCs have SC-like characteristics in immunohistochemical analysis and RT-PCR study of P0. We transplanted BMSC-SCs into the injured rat spinal cord, and performed immunohistochemical studies 5 weeks after transplantation. Transplanted BMSC-SCs maintained the spindle shape and immunohistochemical characteristics of SCs (P0, S100, and p75NTR). In our previous report, we showed that BMSC-SC not only has phenotypic similarity with SCs, but also forms myelin in peripheral nerve tissue.[17,44] However, in the present study no myelin was detected on electron microscopy. A pos-